

Parton model to parton theory: simple model theories

Basic ideas on the space-time structure of deeply inelastic scattering (DIS), symbolized in Figs. 2.2 and 2.5, led us to the parton model in Sec. 2.4. However, as we saw in Ch. 5, the leading regions can be more general than those that give the parton model. Indeed, the properties needed for the literal truth of the parton model are violated in any QFT that needs renormalization or that is a gauge theory, or both, like QCD.

Even so, the ideas that led to the parton model (the distance scales, time dilation and Lorentz contraction) are such basic properties that one should expect the parton model to be some kind of approximation to real QCD.

Because of the complications inherent to a sound treatment in QCD, it is useful to build up methodologies step by step. In this chapter, we treat situations where the parton model is correct, which happens in suitable model field theories. For these we will construct a strict field-theoretic implementation of the parton model.

One key result will be operator definitions of the parton distribution functions (parton densities or pdfs). Another result will be light-front quantization, whereby a probability interpretation of a pdf can be completely justified, in those model theories where the parton model is exact.

6.1 Field theory formulation of parton model

DIS concerns electron scattering off a hadronic target, $e + P \rightarrow e + X$, to lowest order in electromagnetism, with kinematic variables and structure functions defined in Sec. 2.3. Our aim is to understand the asymptotics when the momentum transfer Q is much larger than a typical hadronic scale, with the Bjorken variable x held fixed, away from 0 and 1.

In the parton model (Sec. 2.4), the process is treated as being caused by a short-distance scattering of an electron off a parton, i.e., a quasi-free constituent of the target, with the electron-quark scattering taken to lowest order.

We implement the parton-model idea field-theoretically by an assertion that the dominant contribution arises from cut graphs of the form of the “handbag diagram” of Fig. 6.1, with the virtualities of the explicitly drawn quark lines being much less than Q^2 . The methods of Ch. 5 tell us that this is equivalent to the statement that the only leading regions are those also symbolized by Fig. 6.1, where now the lower subgraph consists of lines collinear to the target, and the upper subgraph consists of lines collinear in another direction.

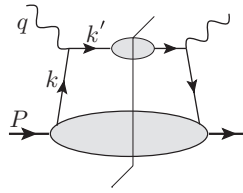


Fig. 6.1. Parton model in field theory starts from “handbag graphs” of this form. The assertion that the parton model is exactly valid is that all leading regions correspond to reduced graphs of the handbag form with the two bubbles being collinear subgraphs.

From the power-counting results in Sec. 5.8 and especially Sec. 5.8.11, we find the conditions that Fig. 6.1 gives all the leading regions: (a) there are no gauge fields, so that no extra gluons connect the hard scattering and the collinear subgraphs, and (b) the theory is super-renormalizable, so that higher-order terms in the hard scattering are power-suppressed.

Evidently, these conditions do not hold in QCD. It is nevertheless useful to investigate the consequences of assuming that Fig. 6.1 gives the whole leading-power behavior of the structure functions.

Even with this restriction, the power-counting results show that leading regions include those with non-trivial corrections on the struck quark line, i.e., that we should use Fig. 6.1 rather than Fig. 2.5(b), where we omitted the upper bubble. The final state for quark k' must therefore be considered a jet of hadrons, in agreement with experiment. The quark k' does not need to give a single particle in the final state; it can only be treated as a single particle over distance scales of order $1/Q$. Of course, if Fig. 6.1 were the whole story, then we would have particles in the final state with fractional electric charge. But Fig. 6.1 is not the whole story, because there are other leading regions in QCD.

6.1.1 Analysis of parton kinematics

We now analyze regions of the form of Fig. 6.1 on the hypothesis that they are the only leading regions. Our aim is to make a formal derivation of the parton model, and to obtain a definition of the parton densities.

It is convenient to use light-front coordinates (App. B) in the Breit frame, as described in Sec. 2.4. (A finite boost will not greatly affect the derivation.) In the Breit frame, the (space-like) photon has zero energy and its large 3-momentum is in the $-z$ direction. Then, as we saw in Sec. 2.4, the big light-front component of the target’s momentum P is the plus component. We define the fractional plus momentum of the incoming quark to be ξ relative to the target, and write

$$q^\mu = \left(-xP^+, \frac{Q^2}{2xP^+}, \mathbf{0}_T \right), \quad (6.1)$$

$$P^\mu = \left(P^+, \frac{M^2}{2P^+}, \mathbf{0}_T \right), \quad (6.2)$$

$$k^\mu = (\xi P^+, k^-, \mathbf{k}_T), \quad (6.3)$$

$$k'^\mu = k^\mu + q^\mu = \left((\xi - x)P^+, \frac{Q^2}{2xP^+} + k^-, \mathbf{k}_T \right), \quad (6.4)$$

with $xP^+ = Q/\sqrt{2}$ in the Breit frame. The collinear property of the momenta is that the only large component of k is its plus component and the only large component of k' is its minus component. From the analysis in Secs. 5.7 and 5.8, we find that the leading contribution is from where the transverse momentum \mathbf{k}_T is of order m , and the small components of longitudinal momentum, k^- and k'^+ , are of order m^2/Q , where m characterizes the particle masses of the theory. Thus $\xi - x$ is of order xm^2/Q^2 .

The contribution of Fig. 6.1 to $W^{\mu\nu}$ is

$$W^{\mu\nu} = \sum_j \frac{e_j^2}{4\pi} \int \frac{d^4k}{(2\pi)^4} \text{Tr} \gamma^\mu U_j(k+q) \gamma^\nu L_j(k, P), \quad (6.5)$$

where $U_j(k')$ and $L_j(k, P)$ are the upper and lower bubbles, which are color- and Dirac-matrix-valued functions of their external momentum and quark flavor. The sum over j is over quark flavors and antiflavors, with e_j being the charge of the struck quark. The trace is over color as well as Dirac indices, and the factor $1/(4\pi)$ is from the definition of $W^{\mu\nu}$.

For the leading power in m/Q , a suitable approximation is to neglect the small components of momentum, k^- , \mathbf{k}_T , and $(\xi - x)P^+$, with respect to Q where possible. A convenient way to do this is:

1. Apply a Lorentz transformation to U so that its quark k' has zero transverse momentum, and then neglect k^- with respect to q^- :

$$\left(k^+ + q^+ - \frac{k_T^2}{2(q^- + k^-)}, q^- + k^-, \mathbf{0}_T \right) \simeq \left(k^+ + q^+ - \frac{k_T^2}{2q^-}, q^-, \mathbf{0}_T \right). \quad (6.6)$$

The matrix for the Lorentz transformation approaches unity as $\mathbf{k}_T/Q \rightarrow 0$.

2. Change the integration variable for the plus component of momentum from k^+ to $l^+ = k^+ + q^+ - k_T^2/2q^-$, so that $k^+ = -q^+ + l^+ + k_T^2/2q^-$. In the region of interest $k^+ \simeq -q^+ = xP^+$, up to a small fractional correction.
3. Therefore, in the lower part of the graph, L , we approximate k^+ by the fixed value xP^+ . For this we need to assume that L is a smooth function of k^+/P^+ , which is normally true in QCD, as evidenced by the smooth dependence of structure functions on x in Fig. 2.6. When the smoothness assumption is false, we can instead apply the derivation to a local average of the x dependence of a structure function, as a generalization of Secs. 4.1.1 and 4.4.
4. Project out the leading part of the Dirac matrix trace.

After the first three steps, we find

$$W^{\mu\nu} \simeq \sum_j \frac{e_j^2}{4\pi} \text{Tr} \gamma^\mu \left[\int \frac{dl^+}{2\pi} U_j(l^+, q^-, \mathbf{0}_T) \right] \gamma^\nu \left[\int \frac{dk^- d^2\mathbf{k}_T}{(2\pi)^3} L_j((xP^+, k^-, \mathbf{k}_T), P) \right]. \tag{6.7}$$

The leading-power approximation has short-circuited the integrations, so that the integrations over k^- and \mathbf{k}_T are restricted to L , and the l^+ integration is restricted to U . So we have two factors coupled by a trace in Dirac spinor space, and a trivial trace over color indices.

6.1.2 Projection of Dirac matrix structure

Projectors on matrix space

To project out the leading part of the Dirac trace, we apply (A.23) to write L in terms of numerical basis matrices:

$$L = A + \gamma_5 B + \gamma_\mu C^\mu + \gamma_\mu \gamma_5 D^\mu + \sigma_{\mu\nu} E^{\mu\nu}, \tag{6.8}$$

where we temporarily drop the flavor index j . Now L is highly boosted from the target rest frame, and we know the transformation properties of the coefficients, which are a Lorentz scalar A , pseudo-scalar B , vector C , etc. In the target rest frame, each of the coefficients $A, \dots, E^{\mu\nu}$ has a fixed order of magnitude. Boosting to the Breit frame increases plus components and decreases minus components by a large factor. The large terms are C^+ , D^+ and E^{+i} , which multiply γ^- factors. Only these can give leading-power contributions to (6.5). They may be obtained from L by, for example, $C^+ = \frac{1}{4} \text{Tr} \gamma^+ L$. Note that the antisymmetry of $\sigma_{\mu\nu}$ removes the possibility of an otherwise dominant term with E^{++} . A similar decomposition applies to U_j , for which the coefficients of γ^+ are biggest.

Projectors on spinor space

The above method works for the quantities L and U as a whole. We now show an alternative method that works more locally in the Feynman graphs: to extract the large Q asymptote, it applies projectors on the individual lines joining the electromagnetic vertices to L and U . This method will show that the hard scattering is computed with Dirac wave functions for on-shell massless quarks, exactly as in the parton model.

Now each of L and U is obtained by a large boost from a rest frame. Since Dirac spinors are in the $(\frac{1}{2}, 0) \oplus (0, \frac{1}{2})$ representation of the Lorentz group, spinors in one two-dimensional subspace increase like $Q^{1/2}$, and those in the other subspace decrease like $Q^{-1/2}$. The first subspace is the part that gives the leading power as $Q/m \rightarrow \infty$. The same subspace is also obtained by taking the zero mass limit, and is the space of Dirac wave functions for the appropriate massless momentum, in the plus direction for L and the minus direction for U .

To project the leading power in the Dirac trace, we therefore use a matrix that projects onto the space of massless wave functions. Let $u_s(p_\infty)$ be a Dirac wave function for a

massless particle of momentum p_∞ and spin label s . A covariantly defined projection onto their space is

$$\mathcal{P}(p_\infty) \stackrel{\text{def}}{=} \frac{\sum_s u_s(p_\infty) \bar{u}_s(p_\infty) \gamma \cdot n}{\bar{u}(p_\infty) \gamma \cdot n u(p_\infty)} = \frac{\not{p}_\infty \gamma \cdot n}{2p_\infty \cdot n}. \tag{6.9}$$

Here n is any vector such that $p_\infty \cdot n \neq 0$.

How do we resolve the ambiguity from the choice of n ? Notice first that $\mathcal{P}(p_\infty)$ is invariant when n is simply scaled by a factor. We actually need a projection matrix for each external line of the hard scattering. The primary constraint on the vector n in each projector is that the projection matrix should not upset the power-counting. Thus if in the center-of-mass frame the largest components of p and n are of order E and n_{max} , then $p_\infty \cdot n$ is at most approximately En_{max} . Preserving the power-counting requires that $p_\infty \cdot n$ should *not* be a large factor smaller than En_{max} . Since the largest component of a on-shell momentum is the energy, it is easiest to satisfy the requirement by setting n to be the rest vector of the center-of-mass.

In the case of DIS, we need two projectors, onto the wave functions for target and jet sides in (6.7). We can choose the n vectors in the $(0, z)$ plane, e.g., the rest vector of the Breit frame. The results are then unique, and the two projectors are

$$\mathcal{P}_A \stackrel{\text{def}}{=} \mathcal{P}(k^+, 0, \mathbf{0}_T) = \frac{\gamma^- \gamma^+}{2}, \quad \mathcal{P}_B \stackrel{\text{def}}{=} \mathcal{P}(0, q^-, \mathbf{0}_T) = \frac{\gamma^+ \gamma^-}{2}. \tag{6.10}$$

For projections onto the conjugate spinors \bar{u} we use

$$\bar{\mathcal{P}}(p_\infty) \stackrel{\text{def}}{=} \frac{n \cdot \gamma \sum_s u_s(p_\infty) \bar{u}_s(p_\infty)}{\bar{u}(p_\infty) n \cdot \gamma u(p_\infty)} = \frac{n \cdot \gamma \not{p}_\infty}{2n \cdot p_\infty} = 1 - \mathcal{P}(p_\infty), \tag{6.11}$$

so that

$$\bar{\mathcal{P}}_A = \mathcal{P}_B, \quad \bar{\mathcal{P}}_B = \mathcal{P}_A. \tag{6.12}$$

Using these in (6.7) to project the leading-power terms gives

$$W^{\mu\nu} \simeq \sum_j \frac{e_j^2}{4\pi} \text{Tr} \gamma^\mu \left[\int \frac{dl^+}{2\pi} \mathcal{P}_B U_j(l^+, q^-, \mathbf{0}_T) \mathcal{P}_A \right] \times \gamma^\nu \left[\int \frac{dk^- d^2\mathbf{k}_T}{(2\pi)^3} \mathcal{P}_A L_j((xP^+, k^-, \mathbf{k}_T), P) \mathcal{P}_B \right]. \tag{6.13}$$

Notice that $\mathcal{P}_A L \mathcal{P}_B$ projects out exactly the terms in L involving C^+ , D^+ and E^{+i} . Thus the projection-matrix technique reproduces the results of the first method in this section.

6.1.3 Parton densities: unpolarized and polarized

We now show how to organize (6.13) into a form involving parton densities and what we will call hard-scattering coefficients. The hard scattering corresponds, as we will see, to

DIS on a free quark target, i.e., the process $\gamma^* + q \rightarrow q$ with the quarks on-shell and of zero transverse momentum.

Definitions

First we define quantities f_j , λ_j and b_{jT}^i by¹

$$f_j(\xi) \stackrel{\text{prelim}}{=} \int \frac{dk^- d^2\mathbf{k}_T}{(2\pi)^4} \text{Tr} \frac{\gamma^+}{2} L_j(k, P), \quad (6.14)$$

$$\lambda_j f_j(\xi) \stackrel{\text{prelim}}{=} \int \frac{dk^- d^2\mathbf{k}_T}{(2\pi)^4} \text{Tr} \frac{\gamma^+}{2} \gamma_5 L_j(k, P), \quad (6.15)$$

$$b_{Tj}^i f_j(\xi) \stackrel{\text{prelim}}{=} \int \frac{dk^- d^2\mathbf{k}_T}{(2\pi)^4} \text{Tr} \frac{\gamma^+}{2} \gamma^i \gamma_5 L_j(k, P), \quad (6.16)$$

with the traces being over both color and Dirac indices. We have a sum over quark colors, and it is not useful to define separate quark densities for different colors. The variable ξ is k^+/P^+ , and is equal to x in the use of these definitions in the parton-model approximation for $W^{\mu\nu}$. We keep the more general variable ξ to emphasize that it is not in the first instance to be identified with the Bjorken x variable of DIS.

These definitions correspond to the leading terms C^+ , D^+ and E^{+i} in (6.8). But there is a change in normalization that lets $f_j(\xi)$ etc. have simple interpretations when we use light-front quantization. We will find that $f_j(\xi)$ is the number density in ξ of quarks of flavor j . The terminology ‘‘parton density’’, ‘‘parton distribution’’ or ‘‘parton distribution function’’ (pdf) is therefore appropriate – all three names are in common use.

We will also find that λ_j is the longitudinal quark polarization and b_{jT} is the transverse quark polarization, both normalized to maximum values of unity. For a spin- $\frac{1}{2}$ parton these variables suffice to specify the most general spin state, pure or mixed; see Sec. 6.5. We will also see that the quark polarizations are functions of ξ times the corresponding variables specifying target polarization. We therefore define the polarized parton densities $\Delta f_j(\xi)$ and $\delta_T f_j(\xi)$ as the coefficients of proportionality:

$$\lambda_{\text{targ}} \Delta f_j(\xi) = \lambda_j f_j(\xi), \quad (6.17)$$

$$\mathbf{b}_{T\text{targ}} \delta_T f_j(\xi) = \mathbf{b}_{Tj} f_j(\xi). \quad (6.18)$$

An interpretation will be that Δf_j is the number density of parallel-helicity quarks minus that of antiparallel-helicity quarks of flavor j in a target of maximal right-handed helicity, i.e., it is the helicity asymmetry. Similarly, $\delta_T f_j(\xi)$ is an asymmetry in transverse spin.

Notation and terminology The transverse spin density is also called the transversity density and the symbols δf , $\Delta_T f$, h_T , $\Delta_1 f$ and h_1 are also used.

¹ The notation $\stackrel{\text{prelim}}{=}$ indicates that these definitions are preliminary. In full QCD, modified definitions will be necessary. The definitions given here are exactly correct only when all of the leading regions in a theory are of the kind depicted in Fig. 6.1.

Parton-model factorization

We now write (6.13) in terms of quark densities and polarization:

$$W^{\mu\nu} \simeq \sum_j \frac{e_j^2}{4\pi} f_j(x) \int \frac{d^4l^+}{\hat{k}^+} \text{Tr}_D \left[\gamma^\mu \mathcal{P}_B U_j(l^+, q^-, \mathbf{0}_T) \mathcal{P}_A \gamma^\nu \frac{\hat{k}}{2} (1 - \gamma_5 \lambda_j - \gamma_5 b_{jT}^i \gamma^i) \right]. \quad (6.19)$$

Here \hat{k} is an approximate version of k ,

$$\hat{k} = (xP^+, 0, \mathbf{0}_T), \quad (6.20)$$

which is massless and of zero transverse momentum. In (6.19), we choose the trace with U to be only over Dirac indices (subscript “D”); a color average is assumed, a triviality since U is a unit matrix in color space. This formula is of the form of a parton density times a structure tensor for DIS on a massless quark target of momentum \hat{k} . It still has an integral over the jet factor U_j , which we will convert to the Dirac matrix for a spin sum for a final-state quark in Sec. 6.1.4.

6.1.4 Result for structure functions; including polarization

We now analyze the jet factor, obtained from the upper part U_j of the graphs. The result will be a cancellation of all but the lowest-order graph, after which we will get exactly the standard parton model result, complete with its generalization to polarized scattering.

To do this, we use an argument from our discussion of e^+e^- annihilation, around Figs. 4.13 and 4.14, applied to the integral over l^+ of

$$\mathcal{P}_B U_j(l^+, q^-, \mathbf{0}_T) \mathcal{P}_A = q^- \gamma^+ \tilde{U}_j(2l^+ q^-), \quad (6.21)$$

which is a cut 2-point function and therefore a discontinuity of an ordinary uncut propagator. In this equation, we have noted that the projectors pick out the coefficient of γ^+ in U , and have observed that its coefficient is q^- times a function \tilde{U} of the virtuality of the quark. Terms proportional to $\gamma^+ \gamma_5$ or to $\gamma^+ \boldsymbol{\gamma}_T$ are absent because of parity invariance and because of rotational invariance of the integral over final states at zero transverse momentum.

Initially we have a contour integral in l^+ around the cut of the propagator. We deform the contour out into complex plane, to where the quark has virtuality $2l^+ q^-$, i.e., of order Q^2 . Here we may correctly approximate all masses in the propagator by zero. Moreover, as usual, the decrease of the projected U (or of the uncut projected propagator) at large l^+ is the decrease of \tilde{U} in (6.21) at large virtuality, which is governed by dimensional analysis of Feynman-graph integrands.

For the moment, we are working under the hypothesis that the parton model is exact, in which case our theory is super-renormalizable. Then all graphs for U beyond lowest order decrease by a power faster than $1/l^+$, and thus they provide a contribution to the integral suppressed by a power of Q . This leaves the lowest-order propagator, which decreases only as $1/l^+$. Therefore, we replace U by the lowest-order cut massless propagator

$\mathcal{P}_B U \mathcal{P}_A = q^- \gamma^+ (2\pi) \delta(2l^+ q^-)$ to obtain

$$\int \frac{dl^+}{\hat{k}^+} \text{Tr}_D \left[\gamma^\mu \mathcal{P}_B U_j(l^+, q^-) \mathcal{P}_A \gamma^\nu \frac{\hat{k}}{2} (1 - \gamma_5 \lambda_j - \gamma_5 s_{jT}^i \gamma^i) \right] = \frac{2\pi}{Q^2} \text{Tr} \gamma^\mu (\hat{k} + q) \gamma^\nu \frac{\hat{k}}{2} (1 - \gamma_5 \lambda_j - \gamma_5 s_{jT}^i \gamma^i). \tag{6.22}$$

Then the parton-model approximation to $W^{\mu\nu}$ is

$$W^{\mu\nu} = \sum_j e_j^2 f_j(x) \left[\frac{1}{2} (-g^{\mu\nu} + q^\mu q^\nu / q^2) + \frac{(\hat{k}^\mu - q^\mu \hat{k} \cdot q / q^2)(\hat{k}^\nu - q^\nu \hat{k} \cdot q / q^2)}{\hat{k} \cdot q} + \frac{1}{2} i \epsilon^{\mu\nu\alpha\beta} \frac{q_\alpha \lambda_j \hat{k}_\beta}{\hat{k} \cdot q} \right]. \tag{6.23}$$

To relate this to our original statement of the parton model, we first recognize the last factor in (6.22) as the numerator factor for DIS on a free massless quark target, i.e., for the process $\gamma^* + q_j(\hat{k}) \rightarrow q_j(\hat{k} + q)$. Next we observe that if we assign the incoming quark a fractional momentum ξ , i.e., if we replace \hat{k} by $(\xi P^+, 0, \mathbf{0}_T)$, then the final-state cut propagator gives a factor

$$2\pi \delta((\hat{k} + q)^2) = \frac{2\pi}{Q^2} x \delta(\xi - x). \tag{6.24}$$

The first factor appears on the right of (6.22), and the delta function sets the parton momentum fraction equal to x .

Comparison of (6.23) with the definitions of the structure functions in (2.20) gives the parton-model results for all four structure functions:

$$F_2^{\text{QPM}} = \sum_j e_j^2 x f_j(x), \quad F_1^{\text{QPM}} = \frac{1}{2} \sum_j e_j^2 f_j(x), \tag{6.25a}$$

$$g_1^{\text{QPM}} = \frac{1}{2} \sum_j e_j^2 \Delta f_j(x), \quad g_2^{\text{QPM}} = 0. \tag{6.25b}$$

The first two agree with the previous results, Bjorken scaling being a prediction. But now we have a concrete derivation, which is susceptible to improvement. We also have a definite definition of the parton densities, and an extension to polarized DIS.

6.1.5 Parton transverse momentum and virtuality

The quark lines entering and leaving the hard scattering have momenta that we approximated as being of zero transverse momentum, massless and on-shell. However, it is important that this is an approximation applied only in a certain part of the diagrams. The actual quarks have non-zero transverse momentum, are off-shell, and have non-zero masses. Thus, in the definition, (6.14) etc., of the parton densities, the parton transverse momentum and virtuality are *non-negligible* and are actually *integrated* over. Failure to recognize this important distinction can lead to all kinds of unphysical paradoxes.

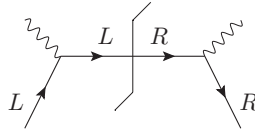


Fig. 6.2. Interference between left-handed and right-handed initial quark in DIS is prevented by helicity conservation at the electromagnetic vertex.

6.1.6 Parton densities vs structure functions

The parton density for transverse spin drops out of the result for $W^{\mu\nu}$, so that the g_2 structure function is zero in the parton-model approximation. This is associated with helicity conservation at the electromagnetic vertex in massless electron-quark scattering, in (6.22). To see this, observe that a transversely polarized state is a linear combination of states of left-handed and right-handed helicity, with a relative phase dependent on the azimuthal angle ϕ of the transverse spin vector around the direction of motion of the particle:

$$|\phi\rangle = \frac{1}{\sqrt{2}} (e^{i\phi/2} |L\rangle + e^{-i\phi/2} |R\rangle). \quad (6.26)$$

Getting a transverse-spin dependence of a cross section, i.e., a dependence on ϕ , requires interference between amplitudes for a left-handed and a right-handed initial state that produce some common final state. But helicity conservation at the electromagnetic coupling of massless particle implies that the final-state quark has the same helicity as the initial state, so that there is no interference (Fig. 6.2).

Because the unpolarized and the longitudinal-polarization quark densities have simple relations to structure functions in the parton model, one often sees a confusion between the concepts of parton density and structure function, with parton densities sometimes being called structure functions. The error of confusing the concepts must be strongly avoided. The structure functions are properties of cross sections, needing only elementary properties of electroweak interactions for their definition. But parton densities are more abstract theoretical constructs in QCD, with definite definitions; they are only related to experiment because factorization theorems can be derived to relate structure functions and other cross sections to parton densities in certain approximations. An excellent example of confusion between parton distributions and structure functions is in Jaffe and Ji (1991), where even the same notation is used for some structure functions and their corresponding parton densities.

The issue becomes particularly noticeable in the case of transverse polarization (Barone, Drago, and Ratcliffe, 2002), since transverse spin dependence drops out of $W^{\mu\nu}$ (at leading power). While the formalism clearly allows for a possible transverse spin dependence, it is the dynamics of a particular theory that determine whether or not there is a non-zero transverse spin dependence for a particular reaction. A reaction other than fully inclusive DIS is needed for a non-zero effect. This has been a topic of intense study in recent years – see Secs. 13.16 and 14.5.4 for examples.

Confusion has arisen from incorrect results in the older literature which apparently indicate that transverse-polarization effects are universally suppressed in hard collisions, contrary to reality. One example is in Feynman (1972), where on p. 157 an incorrect

derivation related a combination of the g_1 and g_2 structure functions to the transverse spin densities. Another example is in Wandzura and Wilczek (1977), where we read (p. 196):

For a highly relativistic quark, the quark spin is, of course, nearly always parallel to its momentum.

and (p. 197):

In the parton model combination $g_1(x) + g_2(x)$ is equal to the difference $k_+(x) - k_-(x)$ of distribution functions for a parton with momentum fraction x in the infinite momentum frame to be spinning up ($k_+(x)$) or down ($k_-(x)$) in a nucleon spinning up (perpendicular to the infinite momentum). Now, again, if the parton is moving rapidly we expect that with overwhelming probability it is spinning along its direction of motion, and therefore

$$k_+(x) \approx k_-(x) \dots$$

Their notation follows that of Feynman (1972), and $k_+(x) - k_-(x)$ is to be identified with $\delta_T f(x)$. The problem is that the large size of the longitudinal component of a boosted spin vector is entirely misleading.

This can be seen in the formula (A.26) for the expression of a spin state in Dirac spinor state. The spin vector appears in the combination \not{S}/M , whose biggest component is of order E/M for a particle of high energy. However the effect of the big component disappears, because it is multiplied by $\not{p} + M$.

This can be seen from the non-singular massless limit (A.27). Thus for our purposes, it is generally preferable to use a helicity density matrix to parameterize the spin state of a particle or a parton (Sec. 6.5). The helicity variable λ is invariant under boosts along the direction of motion. It is true that DIS structure functions on a spin- $\frac{1}{2}$ target are defined, (2.20), in terms of the spin vector; but in a more general situation, the density matrix gives a better route to correct power-counting.

6.2 When is the parton model valid?

The word “valid” in the title of this section means “correct to the leading power of Q ”.

6.2.1 Properties needed to derive parton model

To understand the generalization of the parton model to QCD, it is useful to pinpoint the assumptions used to derive the parton model. Then we can determine QFTs in which the assumptions are derivable or easily repairable. The inter-related assumptions are as follows.

1. The dominant contributions have the structure of Fig. 6.1, i.e., the hard scattering occurs off a single parton, with no final-state interactions between the outgoing parton and the spectator part of the target.

Note that final-state *collinear* interactions of the struck quark are explicitly allowed for, and they cancel, as we showed, so that the final-state quark can be treated as if it were free.

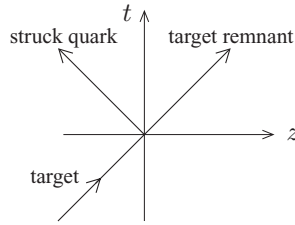


Fig. 6.3. The Libby-Sterman analysis associates these world lines of massless particles in the Breit frame with the leading region that gives the parton model.

2. The hadronic amplitude L falls off sufficiently rapidly at large k_T that the integrals defining the parton densities are convergent.
3. The corrections to U at large virtuality of k' fall more rapidly than the free-field term. Thus when we integrate over the virtuality of k' , as in Sec. 6.1.4, all but the free-field term drop out. This leaves us with an effectively free final-state quark: we can replace Fig. 6.1 by Fig. 2.5(b).
4. The parton density is smooth and slowly varying on a scale of x .

6.2.2 When are they true?

In Secs. 5.8 and 5.9, we found rules that determine all the regions that contribute at the leading power of Q . If all the leading regions are those represented in Fig. 6.1, then we need a super-renormalizable model theory without gauge fields. The lack of gauge fields removes the possibility of a soft subgraph, and of extra gluons connecting the collinear subgraphs to the hard subgraph. Super-renormalizability implies that higher-order corrections to the hard scattering are power-suppressed.

In such a theory (e.g., Yukawa theory in three space-time dimensions) it is also true that the decrease of L at large k_T and of U at large virtuality is sufficient to give convergence of the integrals on the right of (6.13). To see this, we observe that if the integrals did not converge, there would be an unsuppressed contribution from large values of the integration momenta. Then there would be extra leading regions beyond those of Fig. 6.1.

Related to the Libby-Sterman analysis is that the trajectories of the target and its constituents, including the struck quark and the target remnant, are in the vicinity of the light-like world line from bottom left to top right in Fig. 6.3. At the origin, the virtual photon injects negative momentum to make the struck quark go to the left. Near its world line are the collinear interactions that convert the outgoing quark into a jet.

6.2.3 Smoothness or otherwise of parton density

It was known, even in the earliest days, that to derive exactly the parton model from QFT one needs a sufficiently fast decrease of U and L , and that this assumption is violated in typical QFTs in a four-dimensional space-time. However, a less obvious assumption is that the L factor and hence the parton densities are smooth functions of ξ , so that one

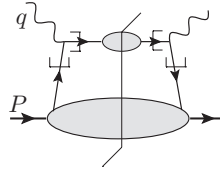


Fig. 6.4. Notation for parton-model approximation to the graph in Fig. 6.1.

can replace k^+ by xP^+ , given that $|k^+ - xP^+| = O(xm^2/Q^2) \ll xP^+$. The necessary quantitative property is that the x derivative of a parton density should obey

$$\left| x \frac{\partial f(x)}{\partial x} \right| \lesssim f(x). \tag{6.27}$$

If this condition is badly violated, the relative errors in the parton-model approximation are much bigger than m^2/Q^2 . When we generalize the parton model to the *standard* factorization theorems of QCD, the same smoothness property is needed.

From experimental measurements, the smoothness property in fact holds at moderate and small x for the real strong interaction, and hence for QCD. This is seen from the plots of the F_2 structure function in Fig. 2.6, or from many successful fits of factorization formulae to data that give measured values for parton densities.

However, the smoothness assumption is not universally true. In the first place, parton densities decrease to zero at $x = 1$ roughly like a power: $f \sim (1 - x)^n$, where the exponent is around 3 to 6, depending on the flavor of parton. Then (6.27) is violated as $x \rightarrow 1$:

$$\left| \frac{x \partial (1 - x)^n \partial x}{(1 - x)^n} \right| = \frac{nx}{1 - x} \sim \frac{n}{1 - x}. \tag{6.28}$$

In the second place, we can apply parton-model methods to other theories. For example in electromagnetic interactions at high energies it can be useful to apply parton methods (and the associated factorization theorems). In that case we need parton densities for electrons and photons in on-shell electron and photon states. As is readily seen in model calculations, these have delta-function terms at $x = 1$. This is the epitome of non-smoothness.

6.2.4 Notation for parton-model approximation

A diagrammatic notation for the approximations used in (6.19) is useful. For an unapproximated graph, Fig. 6.1, we represent the approximation by Fig. 6.4. Crossing the quark lines entering and leaving the hard scattering are thin bent lines (“hooks”) denoting where approximations are applied. The approximations are as follows. On the hard-scattering side, i.e., the concave sides of the hooks, the momenta k and $k' = k + q$ are replaced by $(k^+, 0, \mathbf{0}_T)$ and $(0, k^- + q^-, \mathbf{0}_T)$ respectively, and masses are set to zero (which for this graph is a triviality). Momentum conservation then requires the approximated momenta to equal $(-q^+, 0, \mathbf{0}_T)$ and $(0, q^-, \mathbf{0}_T)$. The approximation also includes the insertion of Dirac projection matrices, \mathcal{P}_A or \mathcal{P}_B , as appropriate.

These operations are all applied on the concave, hard-scattering sides of the hooks. Further operations are applied outside the hard scattering, to change the momentum of the quark in the target bubble from k^+ to $xP^+ = -q^+$, and to change the momentum of the final-state quark so that it has no transverse momentum.

One way of implementing the approximations on momenta is as a replacement of the hard vertex and the associated momentum conservation delta function. Let us use $T_{\text{PM,L}}$ and $T_{\text{PM,R}}$ to denote the application of the approximator on, respectively, the left-hand and right-hand sides of the final-state cut. Because of the Dirac projection matrices, these have slightly different formulae:

$$T_{\text{PM,L}} \gamma^v \delta^{(4)}(q + k - k') = \mathcal{P}_A \gamma^v \mathcal{P}_A \delta(q^+ + k^+) \delta(q^- - k'^-) \delta^{(2)}(\mathbf{k}'_{\text{T}}), \quad (6.29a)$$

$$T_{\text{PM,R}} \gamma^\mu \delta^{(4)}(q + k - k') = \mathcal{P}_B \gamma^\mu \mathcal{P}_B \delta(q^+ + k^+) \delta(q^- - k'^-) \delta^{(2)}(\mathbf{k}'_{\text{T}}). \quad (6.29b)$$

Thus we formulate the approximations locally at the places indicated by the hooks, rather than as global operations on a complete Feynman graph.

6.2.5 Shift of final-state momentum

Our parton-model approximation employed a shift of the plus component of k and the minus component of k' . This implies a shift of the momenta of both parts of the final state, i.e., the target remnant and the struck quark's jet. The approximation is certainly valid under the conditions we consider, i.e., in the parton-model kinematic region, when the parton density is a smooth function of x , and for the fully inclusive structure function, i.e., integrated over hadronic final states.

However, there are more general situations. For example, Monte-Carlo event generators generate complete simulated events for processes like DIS. When they are based on the usual partonic methods, the standard kinematic approximations result in events that violate momentum conservation. Thus it is necessary to adjust (Bengtsson and Sjöstrand, 1988) the parton kinematics so that generated events obey 4-momentum conservation.

In this and similar cases, if one wishes to obtain a more systematic treatment, there is a conflict between the need to maintain exact kinematics and the kinematic approximations used in standard factorization. This has been particularly emphasized by Watt, Martin, and Ryskin (2003, 2004); Collins and Zu (2005); Collins and Jung (2005); Collins, Rogers, and Stašo (2008). These authors show that more general methods are needed. One case, to be treated in this book in Chs. 13 and 14, concerns cross sections sensitive to partonic transverse momentum.

For our immediate purposes, of treating inclusive cross sections, the standard kinematic approximations are appropriate. But it is important to be aware of the flexibility of adjusting the approximations to the actual situations under discussion. Thus it is useful to make very explicit the form of the approximations, with an aim of recognizing situations where changes are needed. The form of the kinematic approximations is closely tied to the detailed structure of the corresponding factorization theorem, and to the definitions of the parton densities (or their generalizations used with different approximations).

6.3 Parton densities as operator matrix elements

6.3.1 Unpolarized quark density

The parton density defined in (6.14) is an integral over the lower bubble in Fig. 6.4, together with a trace with $\gamma^+ / 2$:

$$f_{j/h}(\xi) \stackrel{\text{prelim}}{=} \text{Tr} \frac{\gamma^+}{2} \int \frac{dk^- d^2 k_T}{(2\pi)^4} \text{Diagram} \tag{6.30}$$

where h denotes the type of the target hadron, and $k^+ = \xi P^+$. The diagram is a certain amplitude times its conjugate, with the amplitude involving one off-shell quark, the target state, and a final state. When the quark line on the left of the final-state cut is directed away from the lower bubble, then its top end corresponds to annihilation of a quark by the field ψ_j . It is left as an exercise (problem 6.2) to derive an explicit formula for the quark density as a matrix element of a bilocal operator:

$$f_{j/h}(\xi) \stackrel{\text{prelim}}{=} \int \frac{dw^-}{2\pi} e^{-i\xi P^+ w^-} \left\langle P | \bar{\psi}_j(0, w^-, \mathbf{0}_T) \frac{\gamma^+}{2} \psi_j(0) | P \right\rangle_c \tag{6.31}$$

With standard conventions, it is the *right-hand* part of the matrix element, with the ψ_j field, that corresponds to the part of the diagram to the *left* of the final-state cut, and the left-hand part of the matrix element corresponds to the complex conjugated amplitude on the right of the cut. Only the contribution with the quark fields connected to the target state $|P\rangle$ are to be included, and this is indicated by the subscript “c”.

The field $\psi_j(0)$ represents the extraction of a quark by the hard scattering. Because we integrate over all momentum in the minus and transverse directions, the antiquark field in the complex conjugate amplitude has zero relative position in w^+ and w_T ; note that w^+ is Fourier conjugate to the opposite light-front component k^- in momentum space. The average position of the quark and antiquark fields is irrelevant, since the definition is actually applied to a momentum eigenstate, i.e., a target state uniformly spread out over all space. The space-time locations of the fields are shown in Fig. 6.5.

We have again tagged the definitions as preliminary, in view of the adjustments that will be needed in QCD.

The restriction to connected amplitudes can be implemented by subtracting disconnected graphs, Fig. 6.6, i.e., as subtraction of the vacuum expectation value (VEV) of the operator. This can be written as

$$\langle P' | \bar{\psi}_j(y) \gamma^+ \psi_j(0) | P \rangle_c \stackrel{\text{def}}{=} \langle P' | \bar{\psi}_j(y) \gamma^+ \psi_j(0) | P \rangle - \langle P' | P \rangle \langle 0 | \bar{\psi}_j(y) \gamma^+ \psi_j(0) | 0 \rangle \tag{6.32}$$

An off-diagonal matrix is used here, since momentum eigenstates are non-normalizable. After the subtraction, the diagonal matrix element can be taken: i.e., with $P' = P$. Without this manoeuvre, we would subtract an unquantified infinity proportional to $\langle P | P \rangle$.

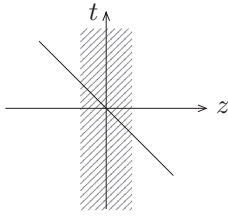


Fig. 6.5. The space-time location of the fields is along a light-like line. The shaded region represents the approximate location of the target hadron in its rest frame.

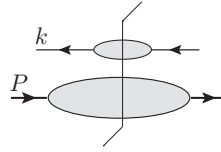


Fig. 6.6. Disconnected graphs, of this form, must be removed from the definition of the parton density when extended to negative ξ .

6.3.2 Antiquark density

For the density of an antiquark, whose flavor we denote by \bar{j} , we have similarly

$$f_{\bar{j}/h}(\xi) \stackrel{\text{prelim}}{=} \int \frac{dw^-}{2\pi} e^{-i\xi P^+ w^-} \text{Tr} \frac{\gamma^+}{2} \langle P | \psi_j(0, w^-, \mathbf{0}_T) \bar{\psi}_{\bar{j}}(0) | P \rangle_c, \tag{6.33}$$

where the trace is over the Dirac and color indices of the fields. In the parton model, the antiquark density appears in contributions to the structure function where the direction of the quark line in Figs. 6.1 and 6.4 is reversed.

6.3.3 Lorentz-covariant definition

The definitions of parton densities are not Lorentz invariant, but they have Lorentz-covariant expressions in terms of a single light-like vector $n^\mu \propto (0, 1, \mathbf{0}_T) = \delta_-^\mu$, so that $\xi = k \cdot n / P \cdot n$. Thus:

$$f_{j/h}(\xi) \stackrel{\text{prelim}}{=} \int \frac{d\lambda}{2\pi} e^{-i\xi n \cdot P \lambda} \left\langle P \left| \bar{\psi}_j(\lambda n) \frac{n \cdot \gamma}{2} \psi_j(0) \right| P \right\rangle_c. \tag{6.34}$$

Here the right-hand side is a scalar, so it is a function of Lorentz invariants only, i.e., of $k \cdot n$ and $P \cdot n$, with n^2 fixed at zero. The formula is invariant under scaling of n by a positive factor, so that only the combination $k \cdot n / P \cdot n$, i.e., ξ , is allowed. Hence, as a function of ξ , the numerical values of the quark density are independent of n , provided only that it is light-like and future-pointing. But for deriving factorization a suitable choice of n is needed, which is determined by the directions of the external momenta p and q .

6.3.4 Relation to wave function?

A parton density can be thought of as some property of the target. But since it is an integral along the light-like line in Fig. 6.5, there can be no simple relation to an ordinary wave function as used in non-relativistic physics, which corresponds to properties of the target at a fixed time in the target rest frame. The transformation to a light-like line involves the interactions of the theory.

We will need to use light-front quantization to interpret parton densities in terms of wave functions (Secs. 6.6 and 6.7).

6.3.5 Support properties

The intermediate state in the parton density, between the two fields, has momentum $P - k$. For it to be physical, it must have non-negative energy, so that $P^+ - k^+ \geq 0$, i.e., $\xi \leq 1$. Thus the parton density is zero if $\xi > 1$.

In the parton-model factorization formula, (6.19) and Fig. 6.4, the final state in the *upper* part of the graph has plus momentum $\xi P^+ + q^+ = (\xi - x)P^+$. This must be positive, in order that the state have positive energy, so that $\xi \geq x > 0$. This restriction applies quite generally in standard factorization formulae for cross sections. Thus we will use parton densities only in the range $0 < \xi \leq 1$.

However, the matrix element for the parton density is generally non-vanishing for negative ξ . We will see later that we can relate $f_{j/h}(\xi)$ for negative ξ to the antiquark density with the opposite sign of ξ : $f_{j/h}(\xi) = -f_{\bar{j}/h}(-\xi)$. This will be critical to the derivation of sum rules. But to make it work, it will be important that we have removed disconnected graphs, Fig. 6.6, from the definition; the disconnected graphs are non-zero for negative values of ξ .

6.3.6 Polarized quark densities

We defined polarized quark densities in (6.15) and (6.16). By the same methods as we used for the unpolarized densities, these can be re-expressed as expectation values in a target state of the operators $\bar{\psi}(z)\gamma^+\gamma_5\psi(0)$ and $\bar{\psi}(z)\gamma^+\gamma^i\gamma_5\psi(0)$:

$$\lambda_{\text{targ}} \Delta f_j(\xi) = \int \frac{dw^-}{2\pi} e^{-i\xi P^+ w^-} \left\langle P, S \left| \bar{\psi}_j(0, w^-, \mathbf{0}_T) \frac{\gamma^+ \gamma_5}{2} \psi_j(0) \right| P, S \right\rangle_c, \quad (6.35)$$

$$\mathbf{b}_{\text{Ttarg}} \delta_T f_j(\xi) = \int \frac{dw^-}{2\pi} e^{-i\xi P^+ w^-} \left\langle P, S \left| \bar{\psi}_j(0, w^-, \mathbf{0}_T) \frac{\gamma^+ \gamma^i \gamma_5}{2} \psi_j(0) \right| P, S \right\rangle_c. \quad (6.36)$$

Here $|P, S\rangle$ denotes a state with normalized helicity λ_{targ} and normalized transverse spin $\mathbf{b}_{\text{Ttarg}}$. These definitions presuppose proportionalities between quark and target spin variables, to be proved in Sec. 6.4. Then the quantities $\Delta f_j(\xi)$ and $\delta_T f_j(\xi)$ are independent of target polarization, i.e., they are parton densities par excellence.

6.3.7 Polarized antiquark densities

Similarly, definitions of polarized antiquark densities are

$$\lambda_{\text{targ}} \Delta f_{\bar{j}}(\xi) = - \int \frac{dw^-}{2\pi} e^{-i\xi P^+ w^-} \left\langle P, S \left| \psi_j(0, w^-, \mathbf{0}_T) \bar{\psi}_j(0) \frac{\gamma^+ \gamma_5}{2} \right| P, S \right\rangle_c, \quad (6.37)$$

$$\mathbf{b}_{\text{Ttarg}} \delta_T f_{\bar{j}}(\xi) = \int \frac{dw^-}{2\pi} e^{-i\xi P^+ w^-} \left\langle P, S \left| \psi_j(0, w^-, \mathbf{0}_T) \bar{\psi}_j(0) \frac{\gamma^+ \gamma^i \gamma_5}{2} \right| P, S \right\rangle_c. \quad (6.38)$$

Note the extra minus sign in (6.37) compared with the other antiquark densities. For the moment, we can regard this as purely a strange convention. Later we will see that the signs are those needed to give a number-density interpretation.

6.4 Consequences of rotation and parity invariance: polarization dependence

In this section, we examine how parton densities depend on the polarization of the particles and the quarks. This will introduce us to techniques for analyzing the consequences for parton physics of symmetries of QCD, and will justify the definitions given in Secs. 6.3.6 and 6.3.7.

Mental health warning: There are no fixed conventions for the normalizations of many of the objects discussed in this section. The objects concerned range from the definitions even of basic mathematical quantities, like $\epsilon_{\kappa\lambda\mu\nu}$, through the definitions of various kinds of spin vector, to the definitions of structure functions and parton densities. Quantities of the same name and symbol change their normalizations between different papers, even by the same authors. If one needs to make numerical results, it is important to check all conventions very carefully.

The conventions used in this book are defined in Apps. A.7 and A.10.

6.4.1 Polarization state

The target can be polarized, and in the most general case a spin density matrix is needed to specify the polarization state. So the target state $|P, S\rangle$ has an extra argument specifying the polarization. For the general case, this argument can be the density matrix, with respect to some basis. But for massive spin- $\frac{1}{2}$ hadron, like a proton, we can use the covariant spin vector S^μ , as defined in App. A.7. Although our notation, as in (6.35) etc., is as if we are working with pure states, there is actually an implicit trace with a helicity density matrix, as defined in (A.8) and (A.13), to allow the target to be in a mixed state.

A helicity basis is rather natural when we work with high-energy particles or with a massless limit. Helicity states are obtained in the theory of irreducible representations of the Poincaré group for massless particles. Moreover, the chiral symmetry ubiquitous in the massless limit of QCD perturbation theory effectively tells us to treat left-handed and right-handed quarks as if they were separate particles. Even so, transversely polarized quarks, i.e., states that are linear combinations of equal amounts of left- and right-handed components, are allowed physically, and have interesting properties.

When we obtain the most general dependence on target spin, it is important that expectation values as defined by (A.13) have a spin dependence that is linear in the spin vector S . Equally, it is linear in the normalized helicity λ and normalized transverse spin \mathbf{b}_T , as defined in App. A.7. Helicity and transverse spin are well behaved in the massless limit unlike the covariant spin vector, and they apply also to the spin state of a quark parton.

The formula (A.12) for S in terms of \mathbf{b}_T and λ exhibits some oddities in the zero-mass limit. In the rest frame of a massive spin- $\frac{1}{2}$ particle, the spin vector has only a spatial component, which unproblematically corresponds to standard usage in non-relativistic

physics. Boosting along the z axis does not change the transverse component of S , but increases its longitudinal components. In contrast, λ and \mathbf{b}_T are invariant under the boost (except for the obvious change of sign when the direction of motion is reversed!).

But a massless particle has no rest frame. Instead one works either with the helicity density matrix or with its decomposition (A.9) in terms of (\mathbf{b}_T, λ) . The spin vector is useful for a proton but not for an on-shell massless quark such as we use in hard scattering. In contrast, the density matrix and the Bloch vector formalisms work for both quarks and protons.

6.4.2 Rotations about z axis

The definition of what we called the unpolarized quark density $f_j(\xi)$ makes no reference to any azimuthal direction, in the (x, y) plane. Therefore we expect this parton density to be independent of the direction of the transverse spin vector of the target. Since matrix elements are linear in the target's spin vector, this implies that there is no dependence even on the size of the transverse spin vector.

To derive this and similar properties formally, we define an operator $U(\phi)$ on state space that corresponds to a rotation by an angle ϕ around the z axis; its action on a helicity eigenstate is

$$U(\phi) |P, \alpha\rangle = e^{-i\alpha\phi} |P, \alpha\rangle. \quad (6.39)$$

Hence the matrix element of an operator between helicity eigenstates obeys

$$\langle P, \alpha' | \text{op} | P, \alpha \rangle = e^{i(\alpha - \alpha')\phi} \langle P, \alpha' | U(\phi)^\dagger \text{op} U(\phi) | P, \alpha \rangle. \quad (6.40)$$

The combination $U(\phi)^\dagger \text{op} U(\phi)$ is the rotated operator. Of the operators defining the parton densities the following two are rotation invariant: $\bar{\psi}(0, w^-, \mathbf{0}_T) \gamma^+ \psi(0)$ and $\bar{\psi}(0, w^-, \mathbf{0}_T) \gamma^+ \gamma_5 \psi(0)$. From (6.40) follows that their matrix elements are diagonal in helicity eigenstates of the target.

For the case of a spin- $\frac{1}{2}$ target, we can apply the rotation to the spin vector S of a general spin state, (A.13), to get

$$\langle P, \text{rotated } S | \text{op} | P, \text{rotated } S \rangle = \langle P, S | \text{rotated op} | P, S \rangle. \quad (6.41)$$

6.4.3 Implications for unpolarized quark density

Spin- $\frac{1}{2}$ target

We now show that the unpolarized quark density $f_j(\xi)$ defined by (6.31) is independent of the polarization state of a spin- $\frac{1}{2}$ target.

We already proved that the matrix elements of the operator defining the unpolarized parton density are diagonal in helicity. But the transverse part of the spin vector only results in off-diagonal terms in the density matrix, so the unpolarized density is independent of transverse spin.

Now a parity transformation reverses the helicity of a state, but also reverses the 3-momentum. A rotation can then be applied to bring the momentum of the state back to its

original value, and makes no change to the already reversed helicity. Thus we can apply the same method as above, but with $U(\phi)$ replaced by a unitary operator U_P that reverses helicity while preserving P :

$$U_P |P, j\rangle = |P, -j\rangle. \tag{6.42}$$

Since the operator in (6.31) is invariant under U_P , it follows that the unpolarized parton density is the same in states of opposite helicity, in a parity-invariant theory.

For a spin- $\frac{1}{2}$ target there are only two helicity states, so we now have shown that the unpolarized parton density $f_j(\xi)$ is independent of the polarization state.

Higher spin

When the target has spin higher than $\frac{1}{2}$, there is a wider range of possibilities. For example, in a spin-1 target, there is one unpolarized quark density for targets of helicity ± 1 and one for targets of helicity zero. There are corresponding generalizations for the DIS structure functions. See problem 6.8 for an exercise to fill in the details, and see Hoodbhoy, Jaffe, and Manohar (1989) for results on DIS, including several new structure functions.

6.5 Polarization and polarized parton densities in spin- $\frac{1}{2}$ target

To treat the polarized densities in a spin- $\frac{1}{2}$ target, we use its helicity density matrix $\rho_{\alpha\alpha'}(S)$ from (A.9), now written as

$$\rho(S) = \frac{1}{2} (I + \lambda_{\text{targ}} \sigma_z + \mathbf{b}_{\text{Ttarg}} \cdot \boldsymbol{\sigma}), \tag{6.43}$$

where the label ‘‘targ’’ is used to distinguish the spin variables for the target from those for the quark. Expectation values of operators are linear in λ_{targ} and $\mathbf{b}_{\text{Ttarg}}$.

The operator defining the polarized parton density $\Delta f_j(\xi)$ in (6.35) is invariant under rotations around the z axis. Therefore its matrix elements are diagonal in helicity and hence independent of transverse spin, just like the unpolarized density. But unlike that case, the operator has the reversed sign under a parity transformation, as does normalized helicity λ_{targ} . So the analog of (6.41) used with the operator U_P of (6.42) shows that the matrix element of the operator is linear in λ_{targ} , as asserted in the matrix element representation (6.35). Thus all the dependence on target polarization is in the explicit factor of λ_{targ} , so that $\Delta f_j(\xi)$ is polarization independent.

Finally, the remaining parton density $\delta_T f_j(\xi)$ in (6.36) is obtained from the matrix element of an operator $\bar{\psi}_j(0, w^-, \mathbf{0}_T) \frac{\gamma^+ \gamma_\perp^i \gamma_5}{2} \psi_j(0)$ that transforms as a (two-dimensional transverse) vector. Because of the γ_5 factor, it actually transforms as a pseudo-vector, i.e., under a parity transformation it acquires a minus sign relative to the transformation of an ordinary momentum. The transverse spin vector is also a pseudo-vector.

To get the correct rotation properties, the matrix element of the operator must be a coefficient times the transverse spin vector, but possibly with the application of a rotation of some angle around the z axis. This rotation, as a function of ξ , would be a property

of the target; it would represent some analog of optical rotation phenomena in a chiral medium. But let us apply a parity transformation followed by a 180° rotation about the x axis (say). This preserves the momentum and the x component of spin of the target, but it reverses the y component of spin. The same transformation applies to the operator. Thus a spin in the x direction gives only a non-zero x component to the matrix element, and similarly for the y component. Thus parity invariance requires there to be exactly no rotation between the spin vector and the matrix elements. (Actually a 180° rotation is also allowed, but for the two transverse directions in question, this is equivalent to a reversal of sign, i.e., to an overall coefficient.) Thus all the dependence on target polarization is in the explicit factor of $\mathbf{b}_{\text{Target}}$, so that $\delta_T f_j(\xi)$ is polarization independent.

6.6 Light-front quantization

A standard method of formulating quantum field theory uses the usual canonical quantization rules for a quantum theory: equal-time commutation (or anticommutation) relations are obtained from the Lagrangian density, and then the Heisenberg equations of motion determine the fields at all times from their values at one particular time. An alternative, first proposed by Dirac (1949), is to use a light-like surface $t + z = 0$ as the initial surface on which (anti)commutation relations are fixed. This is called light-front quantization, with the terms “light-cone quantization” and “null-plane quantization” being synonyms.

Light-front quantization is useful for DIS and other processes where a target system is probed along an almost light-like surface. Inspired by initial approaches using the so-called “infinite momentum frame”, Bardakci and Halpern (1968) developed light-front quantization in field theories. Then Kogut and Soper (1970) made a very clear fundamental treatment. See Brodsky, Pauli, and Pinsky (1998) and Heinzl (2001) for reviews. See also Heinzl and Werner (1994) for a careful treatment of the issue that in solving the equations of motion, it is not sufficient to specify initial conditions on a light-like surface.

As we will now show, light-front quantization gives a direct probability interpretation of parton densities and yields a convenient decomposition of hadronic states in terms of partonic states. Further advantages are explained in the literature just quoted. In extending the method to theories like QCD that are renormalizable or have gauge fields, there are a number of complications that imply that light-front quantization must be used with care. Nevertheless, it provides important insights.

6.6.1 Formulation

To understand the general principles of light-front quantization, we examine the simple case of a Yukawa field theory with Lagrangian density

$$\mathcal{L} = \frac{i}{2} [\bar{\psi} \gamma^\mu \partial_\mu \psi - (\partial_\mu \bar{\psi}) \gamma^\mu \psi] - M \bar{\psi} \psi + \frac{1}{2} (\partial\phi)^2 - \frac{m^2}{2} \phi^2 - g \bar{\psi} \psi \phi - \frac{h}{3!} \phi^3 - \frac{\lambda}{4!} \phi^4. \quad (6.44)$$

This theory is renormalizable at space-time dimension $n = 4$, and is super-renormalizable when $n < 4$. We use the scalar rather than the pseudo-scalar coupling for the Yukawa interaction, to avoid complications with γ_5 in dimensional regularization.

We use light-front coordinates (x^+, x^-, \mathbf{x}_T) as defined in App. B. Then the equations of motion are

$$0 = i\not{\partial}\psi - M\psi - g\psi\phi, \tag{6.45}$$

$$0 = 2\partial_+\partial_-\phi - \nabla_T^2\phi + m^2\phi + g\bar{\psi}\psi + \frac{\hbar}{2}\phi^2 + \frac{\lambda}{3!}\phi^3. \tag{6.46}$$

In light-front quantization we treat these equations as giving evolution in x^+ from fields on the initial surface $x^+ = 0$.

Now the term with an x^+ derivative of the Dirac field is $i\gamma^+\partial_+\psi$, which only affects two independent components of ψ . Therefore we project onto what are called “good” and “bad” components of ψ by the matrices

$$\mathcal{P}_G = \frac{1}{2}\gamma^-\gamma^+, \quad \mathcal{P}_B = \frac{1}{2}\gamma^+\gamma^-. \tag{6.47}$$

These are exactly the same as we used in projecting out the leading power of Q in the Dirac trace in the parton-model approximation to DIS, but now they appear with a more fundamental significance. In view of the jargon of this part of the subject, I replaced the subscript “A” by “G” for good: $\mathcal{P}_G = \mathcal{P}_A$. These matrices obey the usual properties of projectors ($\mathcal{P}_G + \mathcal{P}_B = 1$, $\mathcal{P}_G^2 = \mathcal{P}_G$, etc., and especially $\mathcal{P}_B\mathcal{P}_G = \mathcal{P}_G\mathcal{P}_B = 0$). Then we define the good and bad parts of the fermion field by

$$\psi_G = \mathcal{P}_G\psi, \quad \psi_B = \mathcal{P}_B\psi, \tag{6.48}$$

so that $\bar{\psi}_G = \bar{\psi}\mathcal{P}_B$.

The equation of motion for ψ then separates into two separate two-dimensional pieces:

$$0 = 2i\partial_+\psi_G + \gamma^-(i\gamma^j\nabla_j - M - g\phi)\psi_B, \tag{6.49a}$$

$$0 = 2i\partial_-\psi_B + \gamma^+(i\gamma^j\nabla_j - M - g\phi)\psi_G, \tag{6.49b}$$

where the sums over j are over transverse components. The first equation gives the evolution of ψ_G in x^+ , while we treat the second equation as a constraint: it fixes ψ_B at a given value of x^+ in terms of ψ_G , up to boundary conditions. So we treat ψ_G as the independent set of components. The solution of the constraint equation is

$$\begin{aligned} \psi_B(x) &= \gamma^+ \frac{i}{2\partial_-} (i\gamma^j\nabla_j - M - g\phi)\psi_G \\ &= \frac{i\gamma^+}{4} \int_{-\infty}^{\infty} dy^- \text{sign}(x^- - y^-) (i\gamma^j\nabla_j - M - g\phi)\psi_G(x^+, y^-, \mathbf{x}_T) + C_\psi(x^+, \mathbf{x}_T). \end{aligned} \tag{6.50}$$

There is a term C_ψ independent of x^- that is not determined by the equation of motion. When a Fourier transform over x^- and \mathbf{x}_T is made, to momentum variables k^+ and \mathbf{k}_T , the C_ψ term is proportional to a delta function at $k^+ = 0$. It is therefore characterized as contributing to the zero mode only. A similar zero mode arises in using the equation of motion (6.46) for the ϕ field to determine $\partial\phi/\partial x^+$ in terms of the fields on a surface of fixed x^+ .

The zero-mode issue is quite important to the vacuum structure, and it is not clear to me that it has been properly treated in the literature. But much of what we do will not need a professional treatment of the zero modes. The primary issue is that the equations of motion alone are not sufficient to determine the evolution in x^+ . Extra boundary conditions must be imposed. In contrast, for equal-time quantization, the Euler-Lagrange equations are sufficient to determine the time derivatives of the fields in terms of the independent fields and canonical momentum fields. A related complication concerns the $1/k^+$ singularity in mode sums like (6.59). For treatments of these and related issues, see Nakanishi and Yamawaki (1977), Yamawaki (1998), Heinzl (2003), Heinzl and Ilderton (2007, Sec. 4), and Steinhardt (1980).

We now arrange to form the quantum mechanics of our system by using Hamilton methods, but with evolution in the variable x^+ instead of conventional time.² For this we need commutation relations on surfaces of constant x^+ , and a Hamilton to control the evolution by the standard Heisenberg equation

$$i \frac{\partial A(x)}{\partial x^+} = [A(x), P_+], \quad (6.51)$$

which applies to any field operator $A(x)$. Now the Lagrangian is linear in derivatives with respect to x^+ , so the standard elementary rules of quantization need generalization, for which we use the simple formulation given by Faddeev and Jackiw (1988).

The appropriate Hamilton is just the Noether charge for translations in the x^+ direction, i.e., the appropriate component of momentum:

$$P_+ = \int dx^- d^2\mathbf{x}_T \left[\bar{\psi} (-i\gamma^- \partial_- \gamma - i\gamma^j \nabla_j + M + g\phi)\psi + \frac{1}{2}(\nabla_T\phi)^2 + \frac{m^2}{2}\phi^2 + \frac{h}{3!}\phi^3 + \frac{\lambda}{4!}\phi^4 \right]. \quad (6.52)$$

As with conventional equal-time quantization, for which the founding papers are Born and Jordan (1925); Dirac (1926) and Born, Heisenberg, and Jordan (1926), the equal- x^+ commutation/anticommutation are to be such that the equation of motion in the Heisenberg form (6.51) and in the Euler-Lagrange form (6.46) and (6.49) are equivalent. Thus we have

$$\frac{\partial}{\partial x^-} [\phi(x^+, x^-, \mathbf{x}_T), \phi(x^+, w^-, \mathbf{w}_T)] = \frac{-i}{2} \delta(x^- - w^-) \delta^{(2)}(\mathbf{x}_T - \mathbf{w}_T), \quad (6.53)$$

$$[\psi_G(x^+, x^-, \mathbf{x}_T), \bar{\psi}_G(x^+, w^-, \mathbf{w}_T)]_+ = \frac{\gamma^-}{2} \delta(x^- - w^-) \delta^{(2)}(\mathbf{x}_T - \mathbf{w}_T), \quad (6.54)$$

² For this reason, x^+ and the evolution operator P_+ are sometimes called “light-front time” and “light-front Hamiltonian”.

with the other commutators involving ϕ , ψ_G and $\overline{\psi}_G$ being zero. The subscript + in $[\psi, \overline{\psi}]_+$ etc. denotes the anticommutator appropriate for fermionic fields. Now the first of the above equations is the derivative of the commutator of the scalar field. From it we obtain the commutator of the field with itself:

$$[\phi(x^+, x^-, \mathbf{x}_T), \phi(x^+, w^-, \mathbf{w}_T)] = \frac{-i}{4} \text{sign}(x^- - w^-) \delta^{(2)}(\mathbf{x}_T - \mathbf{w}_T), \quad (6.55)$$

with the boundary condition for inverting $\partial/\partial x^-$ being determined by the antisymmetry of the commutator of two ϕ fields under exchange of the position arguments.

To verify the correctness of this setup, one applies the (anti)commutation relations (6.53) and (6.54) to the the right-hand side of the Heisenberg equations of motion (6.51), for the fields ϕ and ψ_G . In this calculation we do not need the (anti)commutators of ϕ and ψ_G with ψ_B . For example, the term involving $[\phi(x), \psi_B(x^+, y^-, \mathbf{y}_T)]$ is

$$\int dy^- d^2 \mathbf{y}_T [\phi(x), \psi_B(x^+, y^-, \mathbf{y}_T)] \frac{\delta P_+}{\delta \psi_B(x^+, y^-, \mathbf{y}_T)}, \quad (6.56)$$

where $\delta P_+/\delta \psi_B(y)$ denotes a functional derivative. This functional derivative is zero by the constraint equation of motion. It follows from elementary algebra that the Heisenberg equations are also valid for sums and products of fields. Unitary evolution implies that the (anti)commutation relations are true at all x^+ when they are true at $x^+ = 0$.

Since ψ_B is determined from the other fields by the interaction-dependent (6.50), the commutators and anticommutators of ψ_B are interaction dependent. Therefore, because the right-hand side of (6.50) is non-linear in fields, the equal- x^+ (anti)commutators of ψ_B are field dependent. That is, they are not simply numerical-valued functions times the unit operator. This is the primary reason for the jargon of calling ψ_B the bad components of the fermion field. For example, in current algebra one deals with operators constructed out of the elementary fields of a theory. Only for operators constructed solely out of good components at a given value of x^+ can one obtain their commutators directly from the canonical (anti)commutators of the elementary fields, without investigating how to solve the theory.

A similar issue arises with the quark densities. Because of the factor of γ^+ in their defining operators (see (6.31) etc.) only the good components are used:

$$\overline{\psi}(0, w^-, \mathbf{0}_T) \gamma^+ \psi(0) = \overline{\psi}_G(0, w^-, \mathbf{0}_T) \gamma^+ \psi_G(0). \quad (6.57)$$

In Sec. 6.7, we will show that this operator can be represented in terms of light-front annihilation and creation operators for the quark, and this directly gives an interpretation of the quark density as a number density, i.e., as a probability density. This interpretation requires commutation relations for the annihilation and creation operators, which in turn arise from the anticommutation relation (6.54).

It is possible to treat quark correlators constructed from bad components of fields. But the resulting (anti)commutation relations for the Fourier-transformed quantities would be interaction dependent, and hence would be not those of conventional creation and

annihilation operators. Therefore we do not expect any simple interpretation as number densities for parton-density-like quantities constructed using the bad components of the fields.

6.6.2 Light-front annihilation and creation operators

We now obtain annihilation and creation operators in terms of light-front fields (Kogut and Soper, 1970), and derive their commutators.

The annihilation and creation operators are defined by Fourier-transforming the scalar field and the *good* components of the fermion field:

$$\phi(x) = \sum_k \left(a_k(x^+) e^{-ik^+x^- + ik_T \cdot x_T} + a_k(x^+)^\dagger e^{ik^+x^- - ik_T \cdot x_T} \right), \quad (6.58a)$$

$$\psi_G(x) = \sum_{k,\alpha} \left(b_{k,\alpha}(x^+) u_{k,\alpha} e^{-ik^+x^- + ik_T \cdot x_T} + d_{k,\alpha}(x^+)^\dagger u_{k,-\alpha} e^{ik^+x^- - ik_T \cdot x_T} \right). \quad (6.58b)$$

The sum over α is over the two possible values $\alpha = \pm \frac{1}{2}$ for the “light-front helicity” for the fermion, as defined below. The integral over momentum modes is denoted by \sum_k , and is restricted to $k^+ > 0$:

$$\sum_k \dots \stackrel{\text{def}}{=} \frac{1}{(2\pi)^3} \int_0^\infty \frac{dk^+}{2k^+} \int d^2\mathbf{k}_T \dots \quad (6.59)$$

This is just the normal *Lorentz-invariant* form for the integral over a single particle momentum:

$$\frac{1}{(2\pi)^3} \int_0^\infty \frac{dk^+}{2k^+} \int d^2\mathbf{k}_T \dots = \frac{1}{(2\pi)^3} \int d^4k \delta(k^2 - m^2) \theta(k^0) \dots, \quad (6.60)$$

but without the need to specify the value of the mass. This is an advantage since the physical mass is an interaction-dependent quantity, not known before solving the theory, and moreover the formula applies to quarks and other confined particles that do not have a definite physical mass.

Although the integral is restricted to positive k^+ , Fourier modes with the opposite sign of k^+ are allowed for by using terms with a complex-conjugated exponential in (6.58). The distinction between annihilation operators a_k etc. and creation operators a_k^\dagger etc. is made by the sign of the exponential of x^- . (This contrasts with the situation in the Fourier decomposition of fields in equal-time quantization.)

The Dirac wave functions $u_{k,\alpha}$ are defined to be wave functions for massless particles with zero transverse momentum, which span the space of good components (because $\gamma^- u_{k,\alpha} = 0$). They are normalized to obey

$$\bar{u}_{k,\alpha} \gamma^+ u_{k,\alpha'} = 2k^+ \delta_{\alpha\alpha'}, \quad (6.61)$$

and hence

$$\sum_{\alpha} u_{k,\alpha} \bar{u}_{k,\alpha} = k^+ \gamma^- \tag{6.62}$$

The label α corresponds to “light-front helicity” in the sense that

$$\sigma^{xy} u_{k,\alpha} = 2\alpha u_{k,\alpha}, \tag{6.63}$$

which is exactly normal helicity for particles of zero transverse momentum. (Note that $2\alpha = \pm 1$, that $\sigma^{xy} = \frac{i}{2}[\gamma^x, \gamma^y]$, and that the wave function for an antiquark of helicity α is $u_{k,-\alpha}$, with argument $-\alpha$.)

In (6.58), the x^+ dependence is in the annihilation and creation operators, not in the exponential factor, since the x^+ dependence depends on solution of the interacting theory, which is not a simple linear problem.

Unlike the case of the corresponding decomposition at equal time, the annihilation and creation operators correspond to different Fourier components. Thus we obtain these operators simply by inverting the Fourier transform:

$$a_k(x^+) = 2k^+ \int dx^- d^2\mathbf{x}_T e^{ik^+x^- - ik_T \cdot \mathbf{x}_T} \phi(x), \tag{6.64a}$$

$$b_{k,\alpha}(x^+) = \int dx^- d^2\mathbf{x}_T e^{ik^+x^- - ik_T \cdot \mathbf{x}_T} \bar{u}_{k,\alpha} \gamma^+ \psi(x), \tag{6.64b}$$

$$d_{k,\alpha}(x^+) = \int dx^- d^2\mathbf{x}_T e^{ik^+x^- - ik_T \cdot \mathbf{x}_T} \bar{\psi}(x) \gamma^+ u_{k,-\alpha}. \tag{6.64c}$$

Values of masses do not appear in these formulae, in contrast to the corresponding formulae in equal-time quantization, which involve $E_k = \sqrt{\mathbf{k}^2 + m^2}$. Which value of a mass to use would be unobvious and ambiguous. The possibilities include: the physical mass, the bare mass, and the \overline{MS} renormalized mass, none of which are equal, with the relationships only known after the theory is solved. But we are formulating the Fourier transform before solving the theory.

From (6.64) follow the (anti)commutation relations appropriate for annihilation and creation operators:

$$[a_k, a_l^\dagger] = \delta_{kl}, \quad [b_{k\alpha}, b_{l\alpha'}^\dagger]_+ = [d_{k\alpha}, d_{l\alpha'}^\dagger]_+ = \delta_{kl} \delta_{\alpha\alpha'}, \tag{6.65}$$

where δ_{kl} means $(2\pi)^3 2k^+ \delta(k^+ - l^+) \delta^{(2)}(\mathbf{k}_T - \mathbf{l}_T)$. The other (anti)commutators are zero.

6.7 Parton densities as number densities

From the operator definitions (6.31) etc., we now derive the interpretation of parton densities as number densities, as found by Bouchiat, Fayet, and Meyer (1971) and by Soper (1977). See problem 6.6 for corresponding results for the parton density for a scalar field.

6.7.1 Statement of result

Our field-theoretic analysis of DIS structure functions led us to the formal definition of a parton density by (6.31). But previously, in Sec. 2.4, we had introduced the concept of a parton density rather intuitively as a number density. We now complete the picture by showing that the abstract field-theoretic definition is exactly a number density, defined with the aid of light-front annihilation and creation operators:

$$f_{j/h}(\xi) \stackrel{\text{prelim}}{=} \frac{1}{2\xi(2\pi)^3} \sum_{\alpha} \int d^2k_{\text{T}} \frac{\langle P, h | b_{k,\alpha,j}^{\dagger} b_{k,\alpha,j} | P, h \rangle}{\langle P, h | P, h \rangle}. \quad (6.66)$$

Here we have inserted labels j and h for the quark and target type. The prefactor $1/[2\xi(2\pi)^3]$ is present merely to correspond to our chosen continuum normalization of b and b^{\dagger} operators: The (anti)commutation relations in (6.65) imply that the right-hand side of (6.66) is exactly the number density in ξ of quarks of flavor j in hadron h ; its unweighted integral over ξ is a number of quarks.

In the previous section, we explained light-front quantization in the context of a simple model, whereas in the present section our notation is intended to cover more general theories with more than one flavor of quark. We use the terminology “hadron” for the target state, as is appropriate in QCD. In a general field theory, the target state $|P, h\rangle$ can be any stable single-particle state of definite momentum P , the label h serving to distinguish different stable particles. Similarly the parton label j just refers to any particular field in the theory’s Lagrangian.

We explicitly flag (6.66) as preliminary because of important modifications needed in QCD. Even within a super-renormalizable non-gauge model QFT, where the unmodified parton model is valid, there are two important complications:

- Momentum eigenstates have infinite normalization, so the quotient in (6.66) needs interpretation, in terms of an expectation value in a wave packet state, in the limit of a state of definite momentum – see below.
- Our original operator definition had a subtraction of the VEV of the operator, as indicated by the subscript “c” in (6.31). This will not be relevant for the normal situation of positive ξ .

The number density interpretation immediately suggests several sum rules that we will derive. Simple generalizations of the derivation of (6.66) will give corresponding interpretations for the polarized parton densities, and for the parton densities for antiquarks and for scalar (spin-0) partons.

Finally, this result shows that a parton density is an integral of a number density over parton transverse momentum. It is natural to define an unintegrated density, a density in ξ and k_{T} , by simply deleting the integral over k_{T} . This we will do in Sec. 6.8. Unintegrated densities are important to the treatment of reactions with sensitivity to partonic transverse momentum – see Chs. 13 and 14. The original kind of parton density naturally gets

called an “integrated parton density” whenever the distinction with unintegrated densities is needed.

6.7.2 Wave-packet state

Now we return to the derivation of the number density formula (6.66). We first replace the non-normalizable momentum eigenstate $|P, h\rangle$ by a wave-packet state $|P, h; \Delta\rangle$ whose central value of momentum is P and whose momentum-space width, Δ , we will eventually take to zero. The state is a linear combination of momentum eigenstates:

$$|P, h; \Delta\rangle = \sum_{P'} |P', h\rangle F(P'; P, \Delta), \tag{6.67}$$

which we assume to be normalized:

$$\langle P, h; \Delta | P, h; \Delta \rangle = \sum_{P'} |F(P'; P, \Delta)|^2 = 1. \tag{6.68}$$

A suitable form for the wave function is a Gaussian in rapidity and transverse momentum

$$F(P'; P, \Delta) = \frac{4M^{1/2}(2\pi)^{3/4}}{\Delta^{3/2}} \exp\left[-\frac{(y' - y)^2 M^2}{\Delta^2} - \frac{\mathbf{P}'_{\perp}{}^2}{\Delta^2}\right], \tag{6.69}$$

where M is the mass of the target, and we choose the central value P of momentum to have zero transverse component, as usual. To give the wave function a trivial transformation under boosts in the z direction, it is written as a function of rapidity $y = \frac{1}{2} \ln(P^+/P^-)$. The exact form of the wave function will be irrelevant for our work; all that will matter is the peak value and the width. The theorem to be proved is:

$$f_{j/h}(\xi) \stackrel{\text{prelim}}{=} \lim_{\Delta \rightarrow 0} \sum_{\alpha} \int d^2\mathbf{k}_T \frac{1}{2\xi(2\pi)^3} \langle P, h; \Delta | b_{k,\alpha,j}^\dagger b_{k,\alpha,j} | P, h; \Delta \rangle, \tag{6.70}$$

with $f_{j/h}(\xi)$ defined by (6.31).

6.7.3 Derivation

First we verify that the right-hand side is indeed correctly normalized for a number density in ξ and \mathbf{k}_T . To do this, we integrate the operator $b_{k,\alpha,j}^\dagger b_{k,\alpha,j}/[2\xi(2\pi)^3]$ with a smooth function $t(\xi, \mathbf{k}_T)$ and then check its commutation relation with the $b_{k,\alpha,j}^\dagger$. So we define

$$N_i \stackrel{\text{def}}{=} \int d\xi d^2\mathbf{k}_T t(\xi, \mathbf{k}_T) \frac{1}{2\xi(2\pi)^3} b_{k,\alpha,j}^\dagger b_{k,\alpha,j}. \tag{6.71}$$

Then

$$\begin{aligned}
 [N_l, b_{k,\alpha,j}^\dagger] &= \int d\xi d^2\mathbf{k}_T t(\xi, \mathbf{k}_T) \frac{1}{2\xi(2\pi)^3} b_{k,\alpha,j}^\dagger \delta_{kl} \\
 &= t(k^+/P^+, \mathbf{k}_T) b_{k,\alpha,j}^\dagger.
 \end{aligned}
 \tag{6.72}$$

One implication is that when we set the function t to be unity everywhere, the resulting operator N_1 counts the total number of partons of type j . To see this, we apply $b_{k,\alpha,j}^\dagger$ to an eigenstate of N_1 . The commutation relation (6.72) shows that the resulting state is an eigenstate of N_1 , with an eigenvalue increased by unity.

For the main proof, we first use (6.64b) to express the right-hand side of (6.70) in terms of field operators. Before the integral over quark transverse momentum this gives

$$\begin{aligned}
 &\sum_\alpha \frac{\langle P, \Delta | b_{k,\alpha,j}^\dagger b_{k,\alpha,j} | P, \Delta \rangle}{2\xi(2\pi)^3} \\
 &= \sum_{P'', P'} \frac{2k^+}{2\xi(2\pi)^3} F(P'')^* F(P') \int dw^- dz^- d^2\mathbf{w}_T d^2\mathbf{z}_T \\
 &\quad \times e^{-ik^+(w^- - z^-) + ik_T \cdot (\mathbf{w}_T - \mathbf{z}_T)} \langle P'' | \bar{\psi}_j(0, w^-, \mathbf{w}_T) \gamma^+ \psi_j(0, z^-, \mathbf{z}_T) | P' \rangle \\
 &= \sum_{P'', P'} \frac{P^+}{(2\pi)^3} F(P'')^* F(P') \int dw^- dz^- d^2\mathbf{w}_T d^2\mathbf{z}_T \\
 &\quad \times e^{-ik^+(w^- - z^-) + ik_T \cdot (\mathbf{w}_T - \mathbf{z}_T) + i(P'' - P') \cdot z} \langle P'' | \bar{\psi}_j(w - z) \gamma^+ \psi_j(0) | P' \rangle \\
 &= \sum_{P'} \frac{P^+}{2P'^+(2\pi)^3} |F(P')|^2 \int dw^- d^2\mathbf{w}_T \\
 &\quad \times e^{-ik^+(w^- - z^-) + ik_T \cdot (\mathbf{w}_T - \mathbf{z}_T)} \langle P' | \bar{\psi}_j(w - z) \gamma^+ \psi_j(0) | P' \rangle.
 \end{aligned}
 \tag{6.73}$$

In the first step, we used $\sum_\alpha \gamma^+ u_{k,\alpha} \bar{u}_{k,\alpha} \gamma^+ = 2k^+ \gamma^+$. In the third step we performed the integrals over z^- and \mathbf{z}_T with $w - z$ held fixed; the resulting delta function between P' and P'' removed the P'' integral except for a factor $1/(2P'^+)$ implicit in $\sum_{P''}$. In the above manipulations observe the different kinds of momentum label for the target state. The fixed central value is P and this is used to define $\xi = k^+/P^+$. The other variables P' and P'' are dummy variables of integration.

Taking the limit that the wave function is very narrow gives

$$\begin{aligned}
 &\lim_{\Delta \rightarrow 0} \sum_\alpha \frac{\langle P, \Delta | b_{k,\alpha,j}^\dagger b_{k,\alpha,j} | P, \Delta \rangle}{2\xi(2\pi)^3} \\
 &= \int \frac{dw^- d^2\mathbf{w}_T}{(2\pi)^3} e^{-i\xi P^+ w^- + ik_T \cdot \mathbf{w}_T} \left\langle P | \bar{\psi}_j(0, w^-, \mathbf{w}_T) \frac{\gamma^+}{2} \psi_j(0) | P \right\rangle,
 \end{aligned}
 \tag{6.74}$$

whose right-hand side we will take as the definition, (6.79) below, of a quantity $f_{j/h}(\xi, \mathbf{k}_T)$ that we call the unintegrated quark density, or the transverse-momentum-dependent (TMD) quark density.

Integrating the TMD quark density over \mathbf{k}_T reproduces the definition (6.31) of the integrated density. Thus we obtain both the desired theorem, (6.70), and the natural relation that the integrated density is the integral over \mathbf{k}_T of the unintegrated density:

$$f_{j/h}(\xi) \stackrel{\text{prelim}}{=} \int d^2\mathbf{k}_T f_{j/h}(\xi, \mathbf{k}_T). \quad (6.75)$$

Our derivation does not result in the restriction to connected graphs that was implied by the subscript c in (6.31). We will repair this omission when we discuss support properties of parton densities in Sec. 6.9.3.

In view of the particularly significant complications that arise in QCD in the relation between integrated and unintegrated parton densities, please note that assuming any typical naive generalization of (6.75) to QCD will result in conceptually and phenomenologically wrong results. The literature is rife with such results. See Ch. 13, where we will show how the above derivations are to be generalized.

6.7.4 Interpretation of polarized parton densities

The above derivations can readily be generalized to the polarized quark and antiquark densities. The results are as follows.

The quantity $\Delta f_{j/h}$ is the helicity asymmetry of quarks of flavor j . That is, in a target spin- $\frac{1}{2}$ state of definite helicity,

$$\begin{aligned} \Delta f_{j/h}(x) &= \text{density of quark } j \text{ of helicity parallel to target} \\ &\quad - \text{density of quark } j \text{ of helicity antiparallel to target.} \end{aligned} \quad (6.76)$$

This applies also to the antiquark helicity density defined by (6.37). The minus sign in (6.37) compensates the reversed sign for the helicity dependence in the matrix elements of $\gamma^+\gamma_5$:

$$\bar{u}_{k,\alpha}\gamma^+\gamma_5 u_{k,\alpha'} = 4\alpha k^+\delta_{\alpha\alpha'}, \quad \bar{v}_{k,\alpha}\gamma^+\gamma_5 v_{k,\alpha'} = -4\alpha k^+\delta_{\alpha\alpha'}. \quad (6.77)$$

For transverse-spin dependence, there is no such minus sign in the matrix elements of $\gamma^+\gamma^i\gamma_5$, and therefore no minus sign is needed in the transverse-spin asymmetry of the antiquarks, (6.38). Again it can be checked that

$$\begin{aligned} \delta_T f_{j/h}(x) &= \text{density of quark } j \text{ of spin parallel to target} \\ &\quad - \text{density of quark } j \text{ of spin antiparallel to target,} \end{aligned} \quad (6.78)$$

where the spin- $\frac{1}{2}$ target is now chosen to be fully polarized transversely to its direction of motion.

6.9.2 Lorentz invariance/covariance

The definitions of the pdfs depend on a choice of a coordinate system, where the axes are determined by the scattering process being treated. As we saw in (6.34), integrated parton densities can be given explicitly Lorentz-covariant definitions, by use of an auxiliary light-like vector n .

Unintegrated densities need a second vector for a covariant definition. For this, we let n_B be a future-pointing light-like vector with $n_B \cdot n \neq 0$. Up to irrelevant factors, we interpret n and n_B as defining light-front coordinates: $k^+ = n \cdot k$ and $k^- = n_B \cdot k$. Thus n and n_B point in the minus and plus directions respectively. Then we define longitudinal momentum fraction and covariant transverse momentum by

$$\xi = \frac{k \cdot n}{P \cdot n}, \quad k_T^\mu = k^\mu - n_B^\mu \frac{k \cdot n}{n_B \cdot n} - n^\mu \frac{k \cdot n_B}{n_B \cdot n}, \quad (6.82)$$

so that

$$k_T^2 = -k^2 + \frac{2k \cdot n_B k \cdot n}{n_B \cdot n}. \quad (6.83)$$

The unintegrated density (6.79) is

$$f_{j/h}(\xi, k_T) = \int \frac{d^4 w}{(2\pi)^3} \delta(w \cdot n) e^{-i w \cdot k} \left\langle P \left| \bar{\psi}_j(w) \frac{\gamma \cdot n}{2} \psi_j(0) \right| P \right\rangle_c. \quad (6.84)$$

This is invariant when k is shifted in the n direction: $k \mapsto k + cn$.

It is interesting that n_B does not enter this definition, but only in the definition of the variables in (6.82). This situation changes in a gauge theory, where, as we will see in Ch. 13, the definition of unintegrated densities needs Wilson lines in the operators. (Wilson lines are exponentials of integrals of the gauge field along particular lines.)

6.9.3 Support properties, negative ξ

Between the fields in the definition of a parton density, there is a sum over final states, notated by the cut in (6.30). The states have momentum $P - k$, and physical eigenvalues of the plus momentum are positive, so that $P^+ \geq k^+$. Thus pdfs vanish for $\xi > 1$, no matter whether they are integrated pdfs $f(\xi)$ or unintegrated pdfs $f(\xi, k_T)$.

This argument, by itself, provides no restriction for negative ξ . However, we can (anti)commute the two fields in the definition of the pdfs. Since they are at light-like or space-like separation, their (anti)commutator is just the unit operator times a coefficient (localized at $w^- = w_T = 0$). Since we subtract the vacuum expectation value to get the connected matrix element for the pdf, the unit operator from the (anti)commutator gives no contribution. Thus we get a relation between the quark densities at negative x and the antiquark densities at positive x .

The actual relation has an extra minus sign:

$$f_{j/h}(\xi) = -\bar{f}_{j/h}(-\xi), \quad f_{j/h}(\xi, k_T) = -\bar{f}_{j/h}(-\xi, -k_T). \quad (6.85)$$

When the parton is a fermion (e.g., a normal quark), the minus sign arises because we applied an anticommutator. When the parton corresponds to a scalar, the minus sign arises from an explicit factor of ξ in the definition of the scalar-parton density; see problem 6.6. As an example of a derivation, here is the one for the unintegrated densities of a *charged* scalar parton:

$$\begin{aligned}
 f_s(-\xi, -\mathbf{k}_T) &= -\xi P^+ \int_{-\infty}^{\infty} \frac{dw^- d^2\mathbf{w}_T}{(2\pi)^3} e^{i\xi P^+ w^- - i\mathbf{k}_T \cdot \mathbf{w}_T} \langle P | \phi^\dagger(0, w^-, \mathbf{w}_T) \phi(0) | P \rangle_c \\
 &= -\xi P^+ \int_{-\infty}^{\infty} \frac{dw^- d^2\mathbf{w}_T}{(2\pi)^3} e^{i\xi P^+ w^- - i\mathbf{k}_T \cdot \mathbf{w}_T} \langle P | \phi(0) \phi^\dagger(0, w^-, \mathbf{0}_T) | P \rangle_c \\
 &= -\xi P^+ \int_{-\infty}^{\infty} \frac{dw^- d^2\mathbf{w}_T}{(2\pi)^3} e^{i\xi P^+ w^- - i\mathbf{k}_T \cdot \mathbf{w}_T} \langle P | \phi(0, -w^-, -\mathbf{w}_T) \phi^\dagger(0) | P \rangle_c \\
 &= -f_s(\xi, \mathbf{k}_T).
 \end{aligned}
 \tag{6.86}$$

Since antiparton densities vanish for $\xi > 1$, it immediately follows that all parton densities also vanish for $\xi < -1$.

When the scalar field is a hermitian scalar field, the relation is between the parton density and itself, e.g.,

$$f_{\phi/q}(\xi) = -f_{\phi/q}(-\xi) \quad \text{when } \phi \text{ is hermitian.}
 \tag{6.87}$$

A further insight is from the derivation of the probability interpretation. Let us reverse the order of the steps in (6.73), and apply them for negative ξ . Then in place of an annihilation operator $b_{k,\alpha,j}$ we get a creation operator $d_{-k,-\alpha,j}^\dagger$ at the opposite momentum and helicity and for the opposite quark. But we get the operators in the order $d d^\dagger$. To get them in the standard order for a number operator, we must anticommute them, leaving the matrix element of the operator for the number of antiquarks (apart from a sign). To this is added the expectation value of the anticommutator, which is a c number, and therefore removed by subtraction of the vacuum expectation value.

6.9.4 Time-ordered bilocal operators

The definitions given so far for the parton densities involved a fixed ordering of the operators. In Feynman-graph calculations, there is a sum and integral over the final states between two operators, as indicated by the vertical line in the cut-graph notation. Now ordinary Green functions and Feynman-graph calculations involve a matrix element between an in-state and an out-state. So with the final states made explicit, as in

$$\begin{aligned}
 f_{j/h}(\xi, \mathbf{k}_T) &= \sum_X \int \frac{dw^- d^2\mathbf{w}_T}{(2\pi)^3} e^{-i\xi P^+ w^- + i\mathbf{k}_T \cdot \mathbf{w}_T} \\
 &\quad \times \langle P; \text{in} | \bar{\psi}_j(0, w^-, \mathbf{w}_T) | X; \text{out} \rangle \frac{\gamma^+}{2} \langle X; \text{out} | \psi_j(0) | P; \text{in} \rangle_c
 \end{aligned}
 \tag{6.88}$$

6.9.5 Number sum rules

Suppose there is a conserved quark number, as is the case for each flavor (u , d , etc.) in QCD. Then the total number of quarks minus the number of antiquarks of that flavor should equal the value determined by the flavor content of the target state. In QCD we therefore expect the following sum rules for a proton target:

$$\int_0^1 d\xi [f_{u/p}(\xi) - f_{\bar{u}/p}(\xi)] = 2, \quad (6.91a)$$

$$\int_0^1 d\xi [f_{d/p}(\xi) - f_{\bar{d}/p}(\xi)] = 1, \quad (6.91b)$$

$$\int_0^1 d\xi [f_{j/p}(\xi) - f_{\bar{j}/p}(\xi)] = 0 \quad (\text{other flavors}); \quad (6.91c)$$

and of course a baryon number sum rule:

$$\sum_j \int_0^1 d\xi [f_{j/p}(\xi) - f_{\bar{j}/p}(\xi)] = 3. \quad (6.91d)$$

Obvious changes apply for other target states (e.g., a neutron or a particular nucleus). We now show how these rules (and similar ones in model QFTs) are derived when the parton-model hypotheses are obeyed. The full proof in QCD will involve using the correct definitions and treating renormalization effects, but the final answer is the same.

The basic observation is that when we integrate over all ξ in the definition of a pdf, we get a delta function that sets $w^- = 0$, and the operator becomes a component of the Noether current for quark number. Then we use the fact that parton densities vanish for $|\xi| > 1$ and the relation between parton and antiparton densities to get the sum rule

$$\begin{aligned} \int_0^1 d\xi [f_j(\xi) - f_{\bar{j}}(\xi)] &= \int_{-\infty}^{\infty} d\xi \int \frac{dw^-}{2\pi} e^{-i\xi P^+ w^-} \left\langle P \left| \bar{\psi}_j(0, w^-, \mathbf{0}_T) \frac{\gamma^+}{2} \psi_j(0) \right| P \right\rangle_c \\ &= \frac{1}{2P^+} \langle P | \bar{\psi}_j(0) \gamma^+ \psi_j(0) | P \rangle_c. \end{aligned} \quad (6.92)$$

We now have the expectation value of the plus component of the Noether current for the number of quarks of flavor j . From standard properties of currents, this expectation value is the charge of the state times a factor of twice the momentum of the state, which is canceled in the last line. From this result all the above-listed sum rules follow. The subtraction of the VEV implies that the number density is relative to the vacuum.

6.9.6 Momentum sum rule

A very similar argument gives the momentum sum rule:

$$\sum_{\text{all } j} \int_0^1 d\xi \xi f_j(\xi) = 1. \quad (6.93)$$

Here we weight the number densities of partons by ξ , to give a density of fractional momentum. So the sum rule says that the total fractional momentum carried by partons is unity. Note that the sum is over all flavors of parton, including separate terms for antipartons as well as partons. In our Yukawa model this means fermion, antifermion and scalar partons.

The proof is left as an exercise (problem 6.15). It simply involves converting the sum and integral over parton densities to an expectation value of a certain component of the energy-momentum tensor (relative to the vacuum).

6.9.7 Isospin and charge conjugation relations

Consider a theory with an SU(2) isospin symmetry and quarks, like QCD, where we have u and d quarks, which form an isodoublet, and s and heavier quarks, which are all isosinglet.

In real QCD, isospin symmetry is slightly broken by the different masses of the u and d quarks. By neglecting this breaking, we can obtain relations between parton densities in different targets, which hold to the accuracy that isospin symmetry holds. Unlike the sum rules, these relations are valid point-by-point in x .

We will illustrate this for the important cases of the proton and neutron and for the pions. (Scattering experiments are done with all of these particles.) We will obtain a further set of relations for pions using charge conjugation invariance. The general form of all of these arguments is to insert a symmetry transformation operator U times its inverse next to the target state in the definition of a parton density:

$$\langle P, h | U^\dagger U A U^\dagger U | P, h \rangle = \langle P, h' | A' | P, h' \rangle. \quad (6.94)$$

Here h' labels the state obtained by transforming the target, label h , by transformation U , A is the operator whose matrix element is the parton density, and A' denotes the transformed operator.

Since only the transformation properties under simple symmetries are involved in our derivation, the results apply equally to unintegrated parton densities, as well as the more usual integrated parton densities. As explained in Sec. 6.9.8, the results apply equally to the correct QCD definitions of parton densities, so they are presented in their QCD applications.

Proton and neutron

Physical targets are always eigenstates of I_z . So let us take U to be an operator that exchanges the $I_z = \pm \frac{1}{2}$ elements of an isodoublet. We then get the following relations between parton densities on a neutron and a proton:

$$f_{u/p}(x) = f_{d/n}(x), \quad f_{d/p}(x) = f_{u/n}(x), \quad (6.95a)$$

$$f_{\bar{u}/p}(x) = f_{\bar{d}/n}(x), \quad f_{\bar{d}/p}(x) = f_{\bar{u}/n}(x), \quad (6.95b)$$

$$f_{j/p}(x) = f_{j/n}(x), \quad f_{\bar{j}/p}(x) = f_{\bar{j}/n}(x) \quad (j \text{ is } s, c, \text{ etc.}). \quad (6.95c)$$

In electromagnetic DIS, the structure functions are dominated by the density of the u quark, since it has the larger charge. The above relations allow the use of scattering on a nuclear

target to gain information on $f_{u/n}$ and hence on $f_{d/p}$, the density of the lower-charge quark.

Antiproton

One standard beam particle is the antiproton. Parton densities in the antiproton are related to those in the proton by letting U be the charge conjugation operator. This gives $f_{\bar{j}/\bar{p}}(x) = f_{j/p}(x)$ for all species of parton. Particular cases are

$$f_{u/p}(x) = f_{\bar{u}/\bar{p}}(x), \quad f_{d/p}(x) = f_{\bar{d}/\bar{p}}(x). \quad (6.96)$$

These relations are very important for the phenomenology of data from the Tevatron, which uses proton-antiproton collisions.

Gluon in proton, neutron and antiproton

Since the gluon is its own antiparticle as well as being isosinglet, the gluon density is the same in all the targets we have mentioned:

$$f_{g/p}(x) = f_{g/n}(x) = f_{g/\bar{p}}(x). \quad (6.97)$$

Proton target is default

The combination of all the above results means that we can express results for all kinds of nucleon target in terms of parton densities in the proton. So for real QCD applications, when we write a parton density without a hadron label, e.g., $f_u(x)$, it is to be understood that a proton target is intended.

Densities of definite isospin

It is sometimes convenient to use combinations of parton densities that correspond to isotriplet and isosinglet operators, e.g.,

$$f_{I=0}(x) = f_u(x) + f_d(x), \quad (6.98)$$

$$f_{I=1}(x) = f_u(x) - f_d(x), \quad (6.99)$$

with a proton target understood.

Nuclear targets

Data on non-trivial larger nuclei are often analyzed in terms of parton densities in the constituent proton and neutron; this needs a compensation for nuclear-physics effects in nuclear binding. But it is also possible to treat parton densities on the nucleus as a whole. It is often possible to treat nuclei as approximately or exactly isosinglet, notably for the deuteron. In that case isospin relates u and d quark densities, e.g.,

$$f_{u/D}(x) = f_{d/D}(x), \quad f_{\bar{u}/D}(x) = f_{\bar{d}/D}(x). \quad (6.100)$$

(See Schienbein *et al.*, 2009; Eskola, Paukkunen, and Salgado, 2009.)

Pion

The three pions, π^+ , π^- , and π^0 , are related by both isospin and charge conjugation. We leave as an exercise to derive

$$f_{u/\pi^+}(x) = f_{d/\pi^-}(x) = f_{\bar{d}/\pi^+}(x) = f_{\bar{u}/\pi^-}(x), \quad (6.101a)$$

$$f_{d/\pi^+}(x) = f_{u/\pi^-}(x) = f_{\bar{u}/\pi^+}(x) = f_{\bar{d}/\pi^-}(x), \quad (6.101b)$$

$$f_{g/\pi^+}(x) = f_{g/\pi^-}(x), \quad (6.101c)$$

$$f_{s/\pi^+}(x) = f_{s/\pi^-}(x) = f_{\bar{s}/\pi^+}(x) = f_{\bar{s}/\pi^-}(x). \quad (6.101d)$$

It can be seen that there are very few independent densities, which considerably assists the analysis of data with pion beams. The parton densities in the π^0 are determined in terms of the above:

$$f_{u/\pi^0}(x) = f_{d/\pi^0}(x) = f_{\bar{d}/\pi^0}(x) = f_{\bar{u}/\pi^0}(x) = \frac{1}{2} (f_{u/\pi^+}(x) + f_{d/\pi^+}(x)), \quad (6.102a)$$

$$f_{g/\pi^0}(x) = f_{g/\pi^+}(x), \quad (6.102b)$$

$$f_{s/\pi^0}(x) = f_{\bar{s}/\pi^0}(x) = f_{s/\pi^+}(x). \quad (6.102c)$$

These last relations are of relatively little use, since we do not normally deal with beams of neutral pions.

6.9.8 Are the sum rules etc. valid in QCD?

The derivations just presented apply as they stand to a theory which is super-renormalizable and contains only fields of spin zero and spin half. Evidently, QCD violates both prerequisites, and later in the book we will make the necessary improvements. But here it is possible to assess the difficulties and to state the extent to which the results presented continue to apply in QCD.

Our specific model field theory was a very simple Yukawa theory with one field of each type, but the principles immediately generalize when there are multiple fields. Thus we were able to conceive of a theory with the same flavor symmetries as QCD, and to prove certain sum rules.

Isospin relations preserved

In Sec. 6.9.7, we derived relations between parton densities for different flavors of parton and hadron. The only properties that were used of the operators defining parton densities were their transformations under charge conjugation and isospin. These properties are entirely unaffected by the changes needed to accommodate renormalization and the use of gauge fields. This will become fully evident when we construct the definitions of parton densities in QCD.

Renormalization

A renormalizable theory, as opposed to a super-renormalizable theory, is exemplified by the Yukawa theory in four space-time dimensions, $n = 4$. All of the above derivations apply when a UV cutoff is applied, for example dimensional regularization with $n = 4 - 2\epsilon$. The fields in the derivations should be bare fields, i.e., the ones with canonical commutation relations. The bare fields are those for which the coefficients of the first term in each line for the right-hand side of (6.44) is exactly as given. We then remove the UV cutoff after applying renormalization.

To implement renormalization, we first relabel all the fields and parameters in (6.44) with a subscript 0, to denote bare quantities, e.g., g_0 . Then we write the bare fields as renormalized fields times “wave-function-renormalization factors”, e.g., $\psi_0 = \psi\sqrt{Z_2}$ with a conventional notation. Thus the Lagrangian density defining the theory becomes

$$\begin{aligned} \mathcal{L} = & \frac{iZ_2}{2} [\bar{\psi}\gamma^\mu\partial_\mu\psi - (\partial_\mu\bar{\psi})\gamma^\mu\psi] - M_0Z_2\bar{\psi}\psi \\ & + \frac{Z_3}{2}(\partial\phi)^2 - \frac{m_0^2Z_3}{2}\phi^2 - g_0Z_2Z_3^{1/2}\bar{\psi}\psi\phi - \frac{h_0Z_3^{3/2}}{3!}\phi^3 - \frac{\lambda_0Z_3^2}{4!}\phi^4. \end{aligned} \quad (6.103)$$

Finally we adjust the bare parameters, g_0 , Z_2 , etc., in an ϵ -dependent way to remove the divergences. In perturbation theory, this is implemented by using renormalized couplings and masses, g_R , M_R , etc., and using an expansion of the bare parameters in powers of the renormalized coupling, with coefficients adjusted to cancel the divergences order-by-order.

It is Green functions of the renormalized fields ψ and ϕ that are finite rather than those of the bare fields. So we should define the light-front annihilation and creation operators in terms of the renormalized fields. Then the (anti)commutation relations of these operators are changed by wave function renormalization, as in

$$[a_k, a_l^\dagger] = \delta_{kl}Z_3^{-1}, \quad [b_{k\alpha}, b_{l\alpha'}^\dagger]_+ = [d_{k\alpha}, d_{l\alpha'}^\dagger]_+ = \delta_{kl}\delta_{\alpha\alpha'}Z_2^{-1}, \quad (6.104)$$

since it is the bare fields that obey the canonical (anti)commutation relations. An RG analysis can be used to investigate/compute the true value of the renormalization coefficients when the UV cutoff is removed. Generally, the coefficients in (6.104) diverge to $+\infty$ in this limit, with the (rare) exceptions being if the anomalous dimension of a field vanishes strongly enough at the UV fixed point of the theory. The Källén-Lehmann representation of the propagator tells us that $0 \leq Z_i \leq 1$ when an on-shell renormalization prescription is used, so we expect Z_i^{-1} to go to infinity rather than zero in the UV limit.

As we will see later, there are further UV divergences in the integrated parton densities, beyond those removed by wave-function renormalization. We will also see that renormalized integrated parton densities can be defined by a further kind of renormalization, which is completely analogous to what is done for local composite operators.

Since the finite operators no longer have the standard generalized-harmonic-oscillator (anti)commutation relations, and since renormalization of the integrated parton densities is needed, the strict probability interpretation of the parton densities is lost.

Nevertheless, we will show in Sec. 8.6 that the UV divergences cancel in the sum rules, which remain true in a renormalizable theory.

Gauge theories

We will examine the light-front quantization of gauge theories in Sec. 7.4.

Extending the definitions of parton densities to QCD will require significant modifications to the definitions. These involve insertion of what are called Wilson lines to make them gauge invariant: Sec. 7.5. These will further complicate the probability interpretation of parton densities and their renormalization. Nevertheless, the derivation of the sum rules will still work.

6.9.9 Axial currents; Bjorken sum rule

We derived sum rules that related certain integrals over unpolarized parton densities to expectation values of conserved vector currents. Axial currents are also of interest in QCD, so we now discuss the associated sum rules. Even though our discussion of QCD is only later in this book, we can explain the sum rules without this discussion. We simply assume that the definitions given for parton densities can still be used, and then apply them in a theory with the same flavor symmetries as QCD.

The use of axial currents is rather more tricky than vector currents. One reason is that for the $SU(2) \otimes SU(2)$ symmetry of QCD (broken in the Lagrangian only by light quark masses) there is spontaneous symmetry breaking of the axial part of the symmetry. So the expectation values of the axial currents and hence the right-hand sides of the equivalents of (6.91) are determined by the dynamics of QCD, not by the charges of the target. Some of the currents appear in the coupling of quarks to weak gauge bosons, and the matrix elements can be measured, for example, in semi-leptonic decays of hadrons. A second complication is that the isosinglet axial current has an anomaly and is not prone to easy measurement or prediction. A third complication is that whereas there are conserved vector currents in QCD for each of the heavy quarks, resulting in (6.91d), the conservation laws for the axial currents for heavy quarks are badly broken by quark masses.

An elementary generalization of (6.92) leads to the following result for each quark flavor:

$$\int_0^1 d\xi [\Delta f_j(\xi) + \Delta \bar{f}_j(\xi)] = \frac{1}{2P^+} \langle P | \bar{\psi}_j(0) \gamma^+ \gamma_5 \psi_j(0) | P \rangle_c. \quad (6.105)$$

Note that the antiquark term now has a plus sign instead of the minus sign in the number sum rules. *In some sense* the left-hand side measures the total contribution of quarks and antiquarks of flavor j to the spin of the target. Unlike the case of the quark number currents, the current does not correspond to a conserved charge. So there is no direct determination of the right-hand side (although one can well imagine calculating it non-perturbatively by lattice QCD methods).

For the non-singlet combination, we get

$$\int_0^1 d\xi [\Delta u(\xi) + \Delta \bar{u}(\xi) - \Delta d(\xi) - \Delta \bar{d}(\xi)] = \frac{1}{2P^+} \langle P | \bar{\psi}(0) \gamma^+ \gamma_5 \tau_3 \psi(0) | P \rangle_c, \quad (6.106)$$

where τ_3 is a Pauli matrix acting on the doublet of fields for the u and d quarks. We used the quark symbols to denote their parton densities. The current on the right-hand side is one of the generators of the approximate chiral $SU(2) \otimes SU(2)$ symmetry of QCD. It is also related by an isospin transformation for the axial part of the current which couples the W boson to u and d quarks. The matrix element can therefore be deduced from the rate and angular distribution of neutron decay (to $p + e\bar{\nu}$), presented as a value conventionally denoted by G_A/G_V , whose measured value (Amsler *et al.*, 2008) is 1.2695 ± 0.0029 .

Roughly speaking, the sum rule can be probed in the difference between g_1 structure function on the proton and neutron, for which recent data and an analysis related to the sum rule can be found in Airapetian *et al.* (2007). To indicate the idea, we observe that the parton model approximation to g_1 is

$$g_1(x, Q) = \frac{1}{2} \sum_q e_q^2 [\Delta q(x) + \Delta \bar{q}(x)]. \quad (6.107)$$

Using the isospin relations between the polarized parton densities in the neutron and proton, which are immediate generalizations of (6.95), and then using the sum rule (6.106) we get

$$\int_0^1 dx [g_1^p(x, Q) - g_1^n(x, Q)] = \frac{G_A}{6G_V} \simeq 0.21 \quad (\text{parton model}). \quad (6.108)$$

This is one of two results due to Bjorken that are both called Bjorken sum rules.

6.9.10 Moments

The derivation of (6.92) can be readily extended to general integer moments of parton densities by inserting a factor of ξ^{n-1} on the left-hand side and a suitable sign with the antiquark density. The factor of ξ^{n-1} gives $n - 1$ derivatives with respect to the position w^- and we obtain a matrix element of a local operator:

$$\int_0^1 d\xi \xi^{n-1} [f_j(\xi) + (-1)^n f_{\bar{j}}(\xi)] = \frac{i^{n-1}}{2(P^+)^n} \langle P | \bar{\psi}_j(0) \gamma^+ (\partial^+)^{n-1} \psi_j(0) | P \rangle_c. \quad (6.109)$$

In the early days of the study of DIS, the operator product expansion was used to express moments of the DIS in terms of perturbative coefficients times expectation values of local operators, exactly like those on the right-hand side of the above equation; see Ch. 14 of Collins (1984). (Of course, in QCD we need renormalized, gauge-invariant versions of the operators.)

Equation (6.109) shows how these operators are related to parton densities. The expectation values of local operators are susceptible to calculation by Euclidean lattice Monte-Carlo methods, unlike parton densities, whose operators are strictly Minkowski-space objects.

Thus the equation also provides a way that lattice Monte-Carlo methods can be used to give predictions for properties of parton densities.

6.10 Feynman rules for pdfs

In this section, I show how the definitions of parton densities are to be applied in Feynman-graph calculations, by defining special rules for vertices corresponding to the operators in the definitions of the parton densities. Motivated by applications in QCD, I use the word “quark” to refer to the fermion field in our Yukawa model theory, and to its associated particle.

In (6.30), we saw that a quark density can be expressed as an integral over a cut amplitude. A convenient notation is to write

$$\begin{aligned}
 f(\xi) &= \int \frac{d^4k}{(2\pi)^4} \text{Tr}[\gamma^+ \dots] \dots \\
 &= \int \frac{dk^- d^{2-2\epsilon} \mathbf{k}_T \gamma^+}{(2\pi)^{4-2\epsilon} 2} \dots \\
 &= \int \frac{d^{4-2\epsilon} k}{(2\pi)^{4-2\epsilon}} \frac{\gamma^+}{2} \delta(k^+ - \xi P^+) \dots
 \end{aligned}
 \tag{6.110}$$

which gives the Feynman rule for the operator vertices in an *integrated* unpolarized quark density, in $4 - 2\epsilon$ space-time dimensions. The crosses in the first part indicate the operations that are to be applied to the quark fields to obtain the actual pdf. They denote the integrals over k^- and \mathbf{k}_T and the trace with $\gamma^+/2$. The plus component of the momentum at the quark vertices is fixed to be ξP^+ . In view of the extensive use that is made of dimensional regularization, the vertex is given for a general space-time dimension. Were there a color degree of freedom, there would be an unweighted sum over the colors of the field. The bubble indicates the basic matrix element of the quark fields in an on-shell target state of momentum P .

Generalizations to the polarized parton densities are simply made by changing the factor $\gamma^+/2$ to the appropriate Dirac matrix in the definition of the parton density. Similarly, the definitions for the antiquark densities are made simply by changing the direction of the arrow on the quark line. These are all illustrated in Fig. 6.7. Note that the minus sign in the definition of the helicity density of an antiquark requires a corresponding minus sign in the Feynman rule for the antiquark helicity density.

Further generalizations to TMD densities, e.g., Fig. 6.8, are trivially obtained by deleting the integral over transverse momentum. Generally the context will indicate whether we are using integrated or unintegrated densities, so we make no distinction in the graphical

Quark:		unpol.: $\frac{1}{2}\gamma^+$
		hel.: $\frac{1}{2}\gamma^+\gamma_5$
		tran.: $\frac{1}{2}\gamma^+\gamma^i\gamma_5$

Antiquark:		unpol.: $\frac{1}{2}\gamma^+$
		hel.: $-\frac{1}{2}\gamma^+\gamma_5$
		tran.: $\frac{1}{2}\gamma^+\gamma^i\gamma_5$

Fig. 6.7. Gamma matrix factors for all the unpolarized and polarized quark and antiquark densities. For the helicity densities, the target should be in a state of maximum right-handed polarization. For the transversity densities, the target should be in a state of maximum transverse spin, and the rules listed above will give the transversity densities times a unit vector in the direction of the transverse spin of the target. *Note the minus sign in the definition of the helicity density of an antiquark.* Note also that the quark momentum is assumed to be in the direction of the arrow of the quark line. Thus the momentum for the line at the antiquark density is written as $-k$.

$$\begin{array}{c} \text{(TMD)} \\ \uparrow \\ k \\ \uparrow \\ \downarrow \\ \downarrow \end{array} \begin{array}{c} \diagup \\ \diagdown \end{array} = \int \frac{dk^-}{(2\pi)^{4-2\epsilon}} \frac{\gamma^+}{2} \dots$$

Fig. 6.8. The rule for the vertex, as in (6.110), but for a TMD, or unintegrated, quark density. Note that we have not made any notational distinction between the vertices for integrated and unintegrated densities; generally the distinction can be determined from the context.

notation. The common feature of all the definitions is the unweighted integral over all k^- , so that the field operators in the parton density definition are at equal values of x^+ .

The change to the definition with time-ordered products can be made simply by deleting the symbol for the final-state cut.

6.11 Computational examples

In QCD, parton densities with hadronic targets are strictly non-perturbative objects. But it is useful to examine low-order Feynman-graph calculations of parton densities with the target being an elementary particle of a theory.

So in this section, I present some calculations in the model Yukawa theory used in our treatment of light-front quantization. The calculations introduce the methods in their simplest form, and they enable us to see basic principles without being confused by many of the complications – one might almost say pathologies – that arise in QCD. Moreover, such calculations can be used as self-consistent models for interesting effects in QCD – e.g., Brodsky, Hwang, and Schmidt (2002); Collins (2002). In our model calculations, we

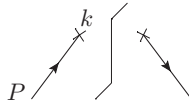


Fig. 6.9. Lowest-order quark density in quark.

will be introduced to the UV divergences of parton densities in renormalizable theories. Perturbative calculations of parton densities also appear as components of perturbative calculations of hard-scattering coefficients.

In the calculations, the target state is a physical on-shell elementary-particle state corresponding to one of the basic field of the theory like the quark. Our calculations in the Yukawa theory of (6.44) are of the density of a quark in a quark, $f_{q/q}(\xi)$, and of a scalar in a quark $f_{\phi/q}(\xi)$.

The concept of the “density of a quark in a quark” is confusing, initially: Why should this not be a trivial delta function at $\xi = 1$? In fact, the word “quark” in that phrase has two meanings. One is for the target state, which is an on-shell physical state. The second meaning is for a state created by the corresponding light-front creation operator. Thus the different instances of the word “quark”, as well as the two instances of the symbol “ q ” in $f_{q/q}(\xi)$, refer to different bases of theory’s state space. In an interacting QFT, on-shell single-particle states, as used in scattering theory, are normally non-trivial combinations of multiparticle states when expressed in the basis given by the creation operators.

6.11.1 Tree approximation

In an expansion in powers of the coupling(s) for $f_{q/q}(\xi)$, the first term is of zeroth order (Fig. 6.9). This is deceptively similar to the representation of just the vertices for the parton density. It is intended to denote the combination of those vertices with the lowest-order amplitude for the bubble in (6.110). The lowest-order bubble consists of $(2\pi)^{4-2\epsilon} \delta^{(4-2\epsilon)}(k - P)$ for momentum conservation in a disconnected graph, and a factor of the on-shell wave function for the target. We allow the most general polarization state for the target, which can be specified by a spin vector S , as in (A.26). We therefore obtain

$$\begin{aligned}
 f_{q/q}^{[0]}(\xi) &= \int \frac{dk^- d^{2-2\epsilon} \mathbf{k}_T}{(2\pi)^{4-2\epsilon}} (2\pi)^{4-2\epsilon} \delta^{(4-2\epsilon)}(k - P) \text{Tr}(\not{P} + M) \frac{1}{2} \left(1 + \gamma_5 \frac{\not{S}}{M} \right) \frac{\gamma^+}{2} \\
 &= \delta(\xi - 1).
 \end{aligned}
 \tag{6.111}$$

Here we use the superscript “[0]” to denote the lowest-order value with zero loops. This calculation provides a basic verification of the normalization of our definition. Without interactions the single on-shell quark is also a single particle in the light-front creation operator basis, and it carries the whole momentum of the target, i.e., it has $\xi = 1$.

6.11.2 One-loop quark in quark

At one-loop order, there are two kinds of graph for $f_{q/q}$ (Fig. 6.10): (a) self-energy corrections on the external line, and (b) a graph with a scalar particle emitted into the final state.

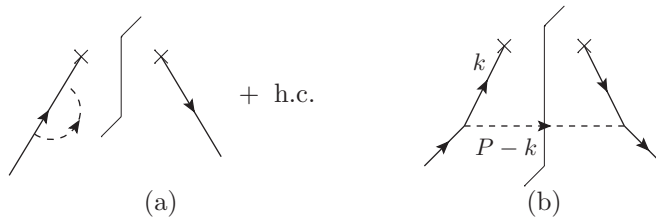


Fig. 6.10. One-loop graphs for density of quark in quark.

(We consider graph (b) a loop graph since there is a momentum integral through the vertex for the parton density.)

Self-energy graph

The full effects of self-energy corrections for external on-shell lines are given by the LSZ method. This tells us that for each external particle we need a factor of the *square root* of the residue of the pole of the propagator. To calculate this, we start from the one-loop self-energy of the quark:

$$\frac{g^2}{16\pi^2} \Sigma^{[1]} = i g^2 \mu^{2\epsilon} \int \frac{d^{4-2\epsilon} k}{(2\pi)^{4-2\epsilon}} \frac{\not{P} - \not{k} + M}{[(P - k)^2 - M^2 + i0](k^2 - m^2 + i0)}. \quad (6.112)$$

The superscript “[1]” denotes the coefficient of the one-loop approximation. As usual, the coupling is written as $g\mu^\epsilon$, where g is dimensionless and μ is the unit of mass for dimensional regularization.

Now the full quark propagator is $i/(\not{p} - M - \Sigma)$. So the one-loop contribution to the residue is given by differentiating $\Sigma^{[1]}$ with respect to \not{p} and by then setting p on-shell. After performing the k integral by the Feynman parameter method, we find that to one-loop order, the residue is

$$1 + \frac{g^2}{16\pi^2} \text{residue}^{[1]} = 1 - \frac{g^2}{16\pi^2} \Gamma(\epsilon) \int_0^1 dx \left[\frac{4\pi\mu^2}{m^2x + M^2(1-x)^2} \right]^\epsilon \times \left[x + \frac{2\epsilon M^2x(1-x^2)}{m^2x + M^2(1-x)^2} \right]. \quad (6.113)$$

We have a factor of the square root of the residue for both external quark lines, so that the resulting one-loop contribution to the quark density is

$$\frac{g^2}{16\pi^2} f_{q/q}^{[1,V]}(\xi) = \delta(\xi - 1) \times \frac{g^2}{16\pi^2} \text{residue}^{[1]}. \quad (6.114)$$

The “V” in the superscript denotes “virtual correction”. Equation (6.113) shows that this contribution is negative. This reduces the size of the one-light-front-particle component in the normalized target state, leaving room for a multiparton component.

Of course, when we go to four space-time dimensions, $\epsilon = 0$, this term is UV divergent. We will explain what happens for the parton density, when we discuss its renormalization.

Real emission

The integral for the real-emission term (Fig. 6.10(b)) is readily written down from the Feynman rules:

$$\frac{g^2}{16\pi^2} f_{q/q}^{[1,R]}(\xi) = g^2 \mu^{2\epsilon} \int \frac{dk^- d^{2-2\epsilon} k_T}{(2\pi)^{4-2\epsilon}} \frac{2\pi \delta((P-k)^2 - m^2)}{(k^2 - M^2)^2} \\ \times \theta(P^+ - k^+) \text{Tr} \frac{\gamma^+}{2} (\not{k} + M)(\not{P} + M) \frac{1}{2} \left(1 + \gamma_5 \frac{\not{P}}{M} \right) (\not{k} + M). \quad (6.115)$$

We set $k^+ = \xi P^+$, and then use the delta function to perform the k^- integral, whereby

$$-2P^+ k^- = \frac{k_T^2 + m^2 - M^2(1 - \xi)}{1 - \xi}. \quad (6.116)$$

This gives

$$\frac{g^2}{16\pi^2} f_{q/q}^{[1,R]}(\xi) = \frac{g^2(4\pi\mu^2)^\epsilon}{16\pi^2 \Gamma(1 - \epsilon)} \int_0^\infty dk_T^2 (k_T^2)^{-\epsilon} \frac{(1 - \xi) [k_T^2 + (1 + \xi)^2 M^2]}{[k_T^2 + \xi m^2 + (1 - \xi)^2 M^2]^2} \\ = \frac{g^2 \Gamma(\epsilon)}{16\pi^2} \left[\frac{4\pi\mu^2}{\xi m^2 + (1 - \xi)^2 M^2} \right]^\epsilon \left[1 - \xi + \frac{\epsilon \xi (1 - \xi) (4M^2 - m^2)}{\xi m^2 + (1 - \xi)^2 M^2} \right]. \quad (6.117)$$

Here, we have used a standard result, (A.34), to perform the angular part of the transverse-momentum integral. The restriction of the final-state momentum $P - k$ to physical positive energy implies that the above formula should have an implicit theta function that restricts it to $\xi \leq 1$. In addition, for negative ξ , as we will see, the calculation is not the complete one; a correct calculation (Sec. 6.11.6) for $\xi < 0$ gives zero. Thus there should also be a restriction to positive ξ . Then in the physical range, we have a non-singular function.

Notice that the denominator is identical to the one in the self-energy. This is related to a cancellation needed to verify sum rules.

Naturally the real-emission contribution is positive, since parton densities are positive, and for the situation that ξ is not equal to unity, our calculation gives the lowest-order contribution.

When the theory is super-renormalizable, in less than four space-time dimensions, i.e., for $\epsilon > 0$, the k_T integral is convergent. But at the physical space-time dimension, with $\epsilon = 0$, there arises a logarithmic divergence at $k_T \rightarrow \infty$. This in fact should be considered a conventional UV divergence, since the virtual line k goes far off-shell, and masses become negligible in the region that gives the divergence. We will discuss the UV divergences later in Sec. 8.3.

6.11.3 One-loop scalar in quark

The remaining one-loop contribution to parton densities in an on-shell quark is the density of the scalar. For this, we need the Feynman rule for the density of a scalar parton (Fig. 6.11).

$$\begin{aligned}
 k \times \int \dots &= \xi P^+ \int \frac{dk^- d^{2-2\epsilon} \mathbf{k}_T}{(2\pi)^{4-2\epsilon}} \text{with } k^+ = \xi P^+ \dots \\
 &= \int \frac{d^{4-2\epsilon} k}{(2\pi)^{4-2\epsilon}} \delta(k^+ / \xi P^+ - 1) \dots
 \end{aligned}$$

Fig. 6.11. Feynman rule for operator for the density of a scalar parton.

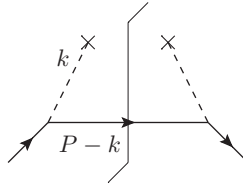


Fig. 6.12. Scalar density in quark.

It has a factor ξP^+ in place of the $\gamma^+ / 2$ for the quark density. The derivation is left as an exercise (problem 6.6), and it results in the definition in (6.124) below.

Then we readily find the one-loop scalar density from Fig. 6.12:

$$\begin{aligned}
 \frac{g^2}{16\pi^2} f_{\phi/q}^{[1]}(\xi) &= g^2 \mu^{2\epsilon} \int \frac{dk^- d^{2-2\epsilon} \mathbf{k}_T}{(2\pi)^{4-2\epsilon}} \frac{2\pi \delta((P - k)^2 - M^2)}{(k^2 - m^2)^2} \\
 &\quad \times \xi P^+ \text{Tr}(\not{P} - \not{k} + M)(\not{P} + M) \frac{1}{2} (1 + \gamma_5 \not{S} / M) \\
 &= \frac{g^2 (4\pi \mu^2)^\epsilon}{16\pi^2 \Gamma(1 - \epsilon)} \int_0^\infty dk_T^2 (k_T^2)^{-\epsilon} \frac{\xi [k_T^2 + (2 - \xi)^2 M^2]}{[k_T^2 + (1 - \xi)m^2 + \xi^2 M^2]^2} \\
 &= \frac{g^2 \Gamma(\epsilon)}{16\pi^2} \left[\frac{4\pi \mu^2}{(1 - \xi)m^2 + \xi^2 M^2} \right]^\epsilon \left[\xi + \frac{\epsilon \xi (1 - \xi)(4M^2 - m^2)}{(1 - \xi)m^2 + \xi^2 M^2} \right]. \quad (6.118)
 \end{aligned}$$

Notice that the denominator is obtained from the denominator in the quark density by changing ξ to $1 - \xi$, as is appropriate now that the scalar line has its plus component of momentum equal to k^+ instead of $P^+ - k^+$. Again, we have a positive contribution, with a UV divergence when $\epsilon = 0$.

The above calculation is valid when $0 < \xi < 1$. As usual, the positive-energy condition on $P - k$ ensures that parton densities are zero if $\xi > 1$. For negative ξ , a more elaborate argument, with extra graphs, is needed, and is given in Sec. 6.11.6.

6.11.4 Sum rules

We now check that the number and momentum sum rules are obeyed by our calculation. Naturally the lowest-order term contributes unity to both the quark number and to the

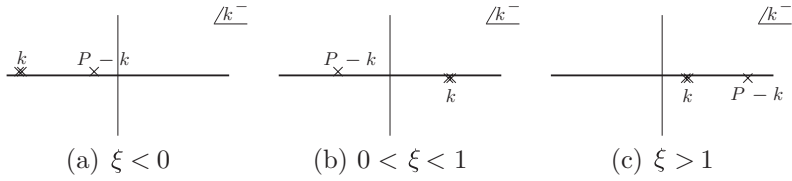


Fig. 6.14. Singularities in k^- plane for (6.121).

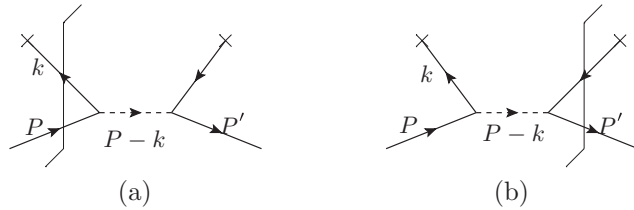


Fig. 6.15. Extra cuts of the one-loop graph for the quark density in a quark. These contribute only for negative ξ , and then cancel the contribution of the standard term Fig. 6.10(b). To avoid a division by zero in the uncut quark propagator, the matrix element is temporarily made off-diagonal in the target momentum.

All the lines now have regular propagators. Notice the overall factor of i compared with (6.115). In terms of light-front coordinates, the denominator factor is

$$\frac{1}{(2\xi P^+k^- - k_T^2 - M^2 + i0)^2 [2(1 - \xi)P^+(P^- - k^-) - k_T^2 - m^2 + i0]}. \tag{6.121}$$

We now perform the integral over k^- by the residue theorem. This works in almost exactly the same way as in Sec. 5.4.2 for the collinear-to- A contribution to the Sudakov form factor. As illustrated in Fig. 6.14, when $\xi < 0$ and when $\xi > 1$ all the poles are in either the upper or lower half plane, so that we can deform the contour to infinity away from the poles and get zero.

The only non-zero contribution is when $0 < \xi < 1$. Closing on the single pole at $(P - k)^2 = m^2$ sets this line on-shell, and exactly reproduces the previous result, (6.117).

6.11.6 Negative ξ

One additional feature of the calculation in the previous section is that a vanishing value is obtained when ξ is negative. From the relation (6.85), this corresponds to a vanishing density of antiquarks in the quark at this order of perturbation theory.

In contrast, in the formalism with fixed ordering for the operators, the cut graph (Fig. 6.10(b)) gives a non-zero value. This appears paradoxical until we observe that there are two further cuts of the same graph, as shown in Fig. 6.15, where the quark propagator is cut, to give a final state consisting of the target and an antiquark of momentum

$-k$. When ξ is positive, the cut lines in Fig. 6.15 do not obey the positive-energy condition for physical particles, and therefore these diagrams give zero. But for negative ξ the positive-energy condition is satisfied, and we get a non-zero contribution from the extra cuts.

A further problem now arises: when we set $k^2 = M^2$ in one quark propagator, the other quark propagator is exactly at its pole and gives infinity. How is one to show in a principled way that the infinities cancel between the two cut graphs in Fig. 6.15 and that the finite part cancels against Fig. 6.10(b)? We could solve this by using a wave-packet state as we did in finding the probability interpretation of parton densities. An alternative, which we will use here, is to start with the matrix element defining the parton density being off-diagonal in target momentum: $\langle P | \dots | P \rangle \mapsto \langle P' | \dots | P \rangle$. We only take the diagonal limit $P' \rightarrow P$ after summing over cuts. The off-diagonal matrix element shifts one of the quark propagators from momentum k to $k + P' - P$, thereby taking the uncut propagator slightly away from its pole. As a function of k^- , the pole and delta function structure for the three cuts is of the form

$$\begin{aligned} & \delta(k^- - A) (-ig) \frac{-i}{k^- - B - i0} (-ig) \frac{-i}{k^- - A' - i0} \\ & + \frac{i}{k^- - A + i0} (ig) \delta(k^- - B) (-ig) \frac{-i}{k^- - A' - i0} \\ & + \frac{i}{k^- - A + i0} (ig) \frac{i}{k^- - B + i0} (ig) \delta(k^- - A'), \end{aligned} \quad (6.122)$$

up to a common overall factor. The quantities A , B and A' are functions of masses, of ξ and the difference between P' and P . The diagonal-matrix-element limit $P' \rightarrow P$ gives $A' \rightarrow A$. Integrating over k^- gives

$$g^2 \frac{1}{A - B} \frac{1}{A - A'} + g^2 \frac{1}{B - A} \frac{1}{B - A'} + g^2 \frac{1}{A' - A} \frac{1}{A' - B}, \quad (6.123)$$

which sums to zero, even before taking the limit $A' \rightarrow A$.

This calculation is a verification in an example of a general result that we proved using operator (anti)commutation relations. The cancellation corresponds to the fact that in the time-ordered-operator formalism, all the poles in the propagators are on one side of the real axis, as in Fig. 6.14(a).

An interesting variant of this problem occurs when we try computing the density of a scalar parton in the fermion target. Exactly the argument we have just given shows that the graph in Fig. 6.12 has two extra cuts and that the sum vanishes for negative ξ . However, we have also shown that, since the scalar particle is its own antiparticle, its density at negative ξ is the negative of the density at positive ξ , (6.87), and therefore is non-zero.

To recover this result, we observe that there are other possible graphs, Fig. 6.16, in which the vertices of the scalar line on the fermion line are reversed. For *positive* ξ , these graphs are zero, and so do not affect the calculation we have already done. But when ξ is in the range $-1 < \xi < 0$, similar arguments to those we gave earlier in this section show that

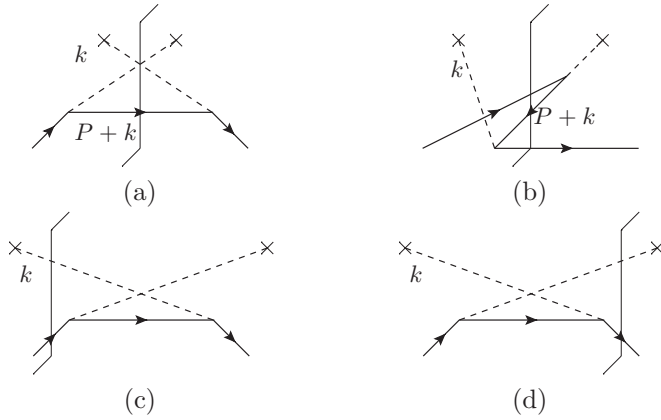


Fig. 6.16. Cut graphs at one-loop order when $\xi < 0$ for the density of scalar partons. Graph (a) is in fact zero, because the coupling of the three on-shell particles violates 4-momentum conservation. Graph (b) only contributes when $\xi < -1$, by the positive-energy condition on the particles on the cut.

the sum of these extra graphs is non-zero, and in fact they result in (6.87). When $\xi < -1$ the graphs sum to zero. Verification of these statements is left as an exercise.

Exercises

- 6.1 Find a/the k_T -dependent Lorentz transformation that converts k to k' in (6.6).
- 6.2 Derive (6.31) from (6.14).
- 6.3 Similarly derive (6.33).
- 6.4 (a) Derive the corresponding results for polarized antiquark densities. Pay careful attention to signs.
 (b) Fill in any other missing details in Sec. 6.5.
- 6.5 What would happen if the theory were parity violating?
- 6.6 (a) Using the methods of this chapter, derive the parton model when the quarks have spin 0. Then derive a formula for the corresponding parton density:

$$f_s(\xi) = \xi P^+ \int_{-\infty}^{\infty} \frac{dw^-}{2\pi} e^{-i\xi P^+ w^-} \langle P | \phi^\dagger(0, w^-, \mathbf{0}_T) \phi(0) | P \rangle_c, \quad (6.124)$$
 including the, perhaps unexpected, factor ξP^+ . [Note: A scalar quark might appear in a model field theory or an extension to QCD, notably a super-symmetric extension.]
 (b) Obtain the corresponding formulae for the unintegrated density.
- 6.7 Carefully derive the signs in the exponents in (6.26).

- 6.8** Generalize whatever needs to be generalized in this chapter to deal with DIS on a spin-1 target like the deuteron. [See Hoodbhoy, Jaffe, and Manohar (1989) for an account of some of the theory, one of the features of which is a new structure function b_1 . See Airapetian *et al.* (2005) for the first measurement of b_1 .]
- 6.9** Check the statement given in the text that, in light-front quantization in the theory specified by (6.44), the standard field equations (6.45) and (6.46) do indeed follow from the canonical (anti)commutation relations (6.53) and (6.54) and the Heisenberg equations of motion (6.51).
- 6.10** Check that the other equations in the sections on light-front quantization and their relations to parton densities are correctly derived, notably (6.65).
- 6.11** Verify the results (6.76) and (6.78) for the interpretation of the polarized parton densities. Do this for both quarks and antiquarks. [Note: There are some subtleties in discussing the spin states needed in the wave-packet derivation that may impinge on this discussion. See Bakker, Leader, and Trueman (2004).]
- 6.12** Generalize the relation between quark for negative ξ and antiquark densities with positive ξ to the polarized case.
- 6.13** Derive the relations (6.101) and (6.102) for parton densities in pions.
- 6.14** Extend these results to kaons.
- 6.15** Generalize the proof in Sec. 6.9.5 to derive the momentum sum rule (6.93). You will need to convert the left-hand side of the sum rule to a matrix element of the energy-momentum tensor.
- 6.16** At one-loop order verify the momentum sum rule (6.93) for a quark target in the Yukawa model theory. The sum over j is over the fermion, the antifermion, and the scalar.
- 6.17** Perform the one-loop calculation of the parton densities for a target that corresponds to the scalar field in our Yukawa field theory. Again verify the momentum sum rule. (The number sum rule is trivially satisfied, since, as you can verify, $f_{\bar{q}/\phi}(\xi) = f_{q/\phi}(\xi)$.)
- 6.18** Verify by explicit calculations the statements at the end of Sec. 6.11.6.
- 6.19** (**) (This problem is quite hard, probably very difficult, and might even deserve three stars.) Suppose we take field theory to be defined by Feynman graphs for Green functions. Derive equal-time and equal- x^+ commutation relations. Thus Feynman perturbation theory does in fact correctly solve the operator formulation of the theory, despite any doubts one might have about the rigor of the derivation of perturbation theory.

Note that there is quite a bit of literature on obtaining commutation relations from time-ordered Green functions, but that most of this dates from the heyday of current algebra and therefore pre-dates QCD. These techniques have not propagated to

modern textbooks. I refer here to the Bjorken-Johnson-Low (BJL) method (Bjorken, 1966; Johnson and Low, 1966).

- 6.20** (***) What happens in the previous problem if you apply it in the presence of renormalization and/or of gauge fields? [Note: Either or both of these conditions is liable to need techniques from the later part of this book, but probably in their simpler forms.]